N 70 27056

NASA CR 66936

Linear and Nonlinear Response of A Rectangular Plate Subjected to Lateral and Inplane Sonic Boom Disturbances.

Report No. 7

Grant NGR-33-013-039

National Aeronautics and Space Administration

April 1970

CASE FILE
COPY

The City College
of
The City University of New York

SCHOOL OF ENGINEERING

DEPARTMENT OF CIVIL ENGINEERING

Linear and Nonlinear Response of A Rectangular Plate Subjected to Lateral and Inplane Sonic Boom Disturbances.

Report No. 7

Grant NGR-33-013-039

National Aeronautics and Space Administration

April 1970

Prepared by Lawrence J. Knapp

Lawrence J. Knapp

David H. Cheng

David H. Cheng

Errata

Pg X change t/t_{11} to τ/τ_{11}

Pg 10 $\tilde{N}_Y + Q_0 \cos 2\eta \geq 0$

Pg 11 equa 2.18

$$T = K_1 e^{d\eta} \sum_{s=-\infty}^{\infty} C_{2s} e^{2si\eta} + K_2 e^{-d\eta} \sum_{s=-\infty}^{\infty} C_{2s} e^{-2si\eta}$$

Pg 14 Table 1, Heading

Initial β check β

Pg 47 Line 1 change Fig. 12 to Fig. 11

3rd P Fig. 13 to Fig. 12

Fig. 14 to Fig. 13

Pg 48 Line 1 Fig. 14 to Fig. 13

2nd P Fig. 15 to Fig. 14

Fig. 13 to Fig. 12

Pg 53 change admissable to admissible

$U = \frac{1}{2} \int_V \sigma_{ij} \epsilon_{ij} \, dV$

Pg 55 Line 4 Fig. 16 to Fig. 15

Fig 11 change R=3 to R=1

Fig 12 change $\bar{w}$ scale to (0.1 to 0.5)

Pg 72 Ref #9 McLachlan, N.W., Theory and Application of Mathieu Functions, Oxford University Press, 1947

TABLE OF CONTENTS

LIST OF TABLES

LIST OF FIGURES

LIST OF FIGURES (continued)

NOMENCLATURE

a, b	Plate length
A_{mn}	Coefficient in Mathieu's equation
$A(\bar{t})$, $B(\bar{t})$, $C(\bar{t})$	Time functions of lateral displacement
B_{mn}	Coefficient in Mathieu's equation
C_{2r}, C_{2r+1}	Coefficient in series solution
Ce_d	Mathieu cosine function of fractional order
$\tilde{C}_r$	Coefficient
d	Order of Mathieu function
D	Flexural rigidity of plate, $Eh^3/12(1-\nu^2)$
DAF	Dynamic amplification factor for stress
E	Young's modulus
f_{mn}	Coefficient in non-homogeneous Mathieu equation
h	Thickness of plate
H	Heaviside function
k	Mass parameter, $M_b/\mu a$
N_x, N_y, N_{xy}	Membrane Stresses
$\tilde{N}_y$	Constant inplane load
N_c	Static buckling load
p_o	Peak overpressure of N-shaped disturbance
q_n	Coefficient in Mathieu's equation
Q_o	Maximum amplitude of dynamic inplane disturbance
Q_c	Current amplitude of dynamic inplane disturbance

S_n	Coefficient in Mathieu's equation
Se_d	Mathieu sine function of fractional order
$\tilde{S}_r$	Coefficient
t	Time
$\bar{t}$	Dimensionless time ratio t/τ_{11}
$\bar{t}_{cr}$	Critical time
t_o	Time delay
$\bar{t}_o$	Dimensionless time delay t_o/τ_{11}
T	Kinetic energy of plate
$\bar{u}$	Dimensionless inplane displacement in x direction
U	Strain energy of plate
$\bar{v}$	Dimensionless inplane displacement in y direction
w	Lateral deflection
$\bar{w}$	Dimensionless lateral deflection
W	External work
$\bar{x}, \bar{y}$	Dimensionless space parameter
α	Coefficient defining duration of dynamic inplane disturbance
α_r	Coefficient
β	Fractional part of d
Δ	Laplacian operator
∇^4	Biharmonic operator

η	Transformed dimensionless time
μ	Mass per unit area of plate
ν	Poisson's ratio
ξ_1, ξ_2	Coefficient
σ_c	Critical stress, N_c/h
σ_d	Dynamic bending stress
σ_s	Static bending stress
σ_y	Membrane stress
τ	Duration of N-shaped disturbance
$\bar{\tau}(=R)$	Dimensionless duraction of N-shaped disturbance, t/t_{11}
τ_{mn}	Natural period of plate
φ_x	Function of time
φ_y	Function of time
ω_o	$\sqrt{Eh/M_b b(1-\nu^2)}$

Abstract

The transient response of a rectangular window pane exposed to a far-field sonic boom disturbance is studied with the help of both the linear and nonlinear theories. The sonic boom disturbance causes a lateral disturbance in the form of an N-shaped pressure pulse and an inplane disturbance in the form of a sinusoidal pulse.

In the linear theory, the imposition of lateral and inplane pulses may be simultaneous or separated by a brief time-delay. In addition there may be a static inplane load. Due to the inplane sinusoidal pulse load, the equation of motion is of the Mathieu type. An improved procedure in solving Mathieu's equation is presented. The effects of the inplane static and dynamic loads, the pulse durations, and the time-lag are studied.

In the nonlinear theory, in addition to the usual simply supported boundary conditions, two sets of inplane boundary conditions are specified: movable vertical sides and immovable vertical sides. For both sets of inplane boundary conditions, the longitudinal inertia of the plate is either neglected or considered by assuming that the longitudinal mass is concentrated at the top of the plate. The equations of motion are reduced to a set of ordinary nonlinear coupled differential equations by using the Galerkin method. These equations are solved numerically by

Hamming's modified predictor-corrector integration method. The effects of the dynamic inplane load, the lateral overpressure, and the movable and immovable vertical sides are studied. A comparison of the results obtained by the linear and nonlinear theories is made.

CHAPTER 1

INTRODUCTION

The effects of sonic boom disturbances on structural elements have been extensively studied in recent years [1]. The disturbance was idealized as an N-shaped pressure wave moving either parallel or normal to the surface of the structural element [2]. The load is therefore laterally applied. One of the most vulnerable structural elements is known to be the plate glass window [3]. Due to a certain unfavorable combination of circumstances, a window pane may be subjected to inplane as well as lateral disturbances. It is conceivable that much higher stress amplitudes may result due to the presence of the additional inplane disturbance.

A rectangular plate subjected to an inplane static load tends to become more flexible if the load is compressive and more rigid if it is tensile. The vibration problems of a rectangular plate with constant inplane static loads and various boundary conditions have been studied rather extensively [4]. The dynamic response of a plate subjected to a steady-state periodic inplane disturbance has also been extensively treated [5][6]. However, the dynamic behavior of a plate subjected to both lateral and inplane disturbances has not appeared in the literature.

When a flat plate is subjected to a steady-state periodic inplane disturbance, the plate may exhibit lateral oscillations. This type of oscillation is induced by what is known as a parametric excitation.

Linear theories can be used to predict the frequency zones for which a lateral parametric excitation may exist. However, nonlinear effects must be included to determine the amplitude of these oscillations.

Using a nonlinear theory, Bolotin [5] presented a one mode solution for the amplitude of the lateral parametric vibrations of a simply supported plate. It was assumed that the longitudinal mass of the plate was small and, therefore, the distributed longitudinal inertia of the plate was neglected. The periodic inplane disturbance was transmitted to the plate by a rigid bar. The problem was solved for a rigid bar that was massless and for a rigid bar which had a distributed mass along it. The principal instability zone was determined as well as the amplitude of the lateral vibrations.

Somerset and Evan-Iwanowski [6], using a large deflection theory, analyzed the same problem using a four mode expansion for the amplitude of the lateral parametric vibrations. There was a distributed mass along the rigid bar on the top and the effects of the distributed longitudinal inertia of the plate were included in the analysis. It was shown that the inplane distributed inertia influences the frequencies associated with the principal instability zone. Further, it was shown that when the mass on the top becomes very large, the solution reduces to that given by Bolotin [5].

It is clear that the primary aim of the above investigations [5] [6] was to study the dynamic stability of the structure under the parametric excitation. The phenomenon of instability is associated with large time. On the other hand the present investigation deals with the dynamic response of a rectangular plate subjected to both inplane and lateral disturbances which are essentially transient in nature.

The rectangular plate under consideration is simply supported along all edges. It is subjected to a lateral disturbance in the form of an N-shaped pressure pulse, and to a dynamic inplane disturbance in the form of a sine pulse (Fig. 1). The imposition of the lateral and inplane disturbances may be simultaneous or separated by a brief time-delay. In addition, there may be a static inplane load (or prestress) in the vertical (y) direction. However, the loading condition at the top of the plate is such that it is incapable of transmitting a tensile load. In other words, the combination of the prestress and the dynamic inplane load can never be in tension and, if the prestress is absent, the sinusoidal inplane pulse has only a compression phase.

The problem is studied first by a small deflection or linear theory. Due to the presence of the inplane dynamic load in the form of a sine pulse, the equations of motion are of the Mathieu type [7]. For the present problem, only the stable solution is of interest. The homogeneous equations are solved by a procedure first suggested by Floquet [8]. Following McLachlan [9], the solution is obtained in terms of Mathieu functions of fractional order. However, it is discovered that the procedure outlined by McLachlan does not always insure an accurate determination of the coefficients in the series solution. An improved procedure is presented in Chapter 2 which removes this drawback. Once the solution to the homogeneous equation is obtained, the particular solution is determined by the method of variation of parameters.

It may be anticipated that the lateral deflection of the plate may reach such a magnitude as to render the results of the linear theory invalid. In that case, the nonlinear plate equations known as the Von Kármán [10] equation must be used to take into account the stretching of the mid-surface of the plate. For this dynamic problem, the equations of motion and the associated boundary conditions can be derived by Hamilton's Principle [11]. The derivation is carried out in the Appendix.

In Chapter 3, the problem is posed for two different inplane boundary conditions: movable vertical sides and immovable vertical sides. Along the top edge of the plate, where the dynamic inplane load is transmitted to the plate, two sets of conditions are specified. One has the longitudinal mass of the plate lumped along a rigid bar and the other a rigid bar with no mass. All the sides of the plate are constrained to remain straight. A three mode expansion for the lateral deflection is proposed. The inplane displacements are determined in terms of the lateral deflection. By using the Galerkin Method [12], the equations of motion governing the lateral deflections are reduced to a set of ordinary differential equations. These equations are coupled and nonlinear, and are solved numerically using Hamming's Modified Predictor-Corrector Integration Technique [13].

In Chapter 4, the solutions based on the linear and nonlinear theories are applied to a square glass plate with the ratio of sides, a, to thickness, h, of 240. The severity of the dynamic response of the plate to the dynamic loadings is studied with the help of a dimensionless quantity known as the dynamic amplification factor for stress (DAF). The DAF is defined as the ratio of the maximum dynamic stress to the maximum static stress. The maximum static stress is obtained on the basis of the small deflection theory when the plate is subjected to the peak pressure of the N-shaped pressure pulse uniformly applied over the plate. It is seen that if the DAF is known for a given plate subjected to the given disturbances, the maximum stress can be easily obtained.

Using the linear theory, the case with no time-lag is considered first, followed by the case with either a positive or a negative time-lag. A positive time-lag means that the lateral disturbance leads the inplane disturbance by a certain time. The effects of the inplane loads (both static and dynamic), the duration of the inplane dynamic load, and the time-delay between the inplane and lateral disturbances are studied.

To simplify the amount of computations in the nonlinear model, the duration of the inplane and lateral disturbances are made the same and the time-lag is not considered. In the case of the movable sides, it is shown that if the prestress is absent the effect of the longitudinal inertia is negligible for the problem studied. The effects of the dynamic inplane load, the overpressure of the N-shaped disturbance, and the movable and immovable vertical sides are studied.

A comparison of the linear and nonlinear theories is made to delineate the validity of the linear theory. For small overpressure, p_o less than 2psf, the deflections obtained by the linear theory are only 10% greater than those of the nonlinear theory.

Chapter 2. Response of Rectangular Plates Based on Small Deflection Theory

a) Formulation of the Problem

Consider a simply supported rectangular plate, of sides a and b, and of uniform thickness h, which is subjected to an inplane as well as a lateral disturbance. The lateral disturbance is characterized by an N-shaped pressure pulse followed with a time delay, t_o, by the inplane disturbance characterized by a single sine pulse. In addition, there is an inplane prestress in the vertical direction, $\tilde{N}_y$. The plate and the disturbances are illustrated in Fig. 1.

The equation of motion of the plate [14] is:

$$D\nabla^4 w + [Q_0 \sin\frac{2\pi}{\alpha\tau}(t-t_o)\, H(t-t_o)\, H(\alpha\tau+t_o-t) + \tilde{N}_y]\, w_{,yy} + \mu \ddot{w} = p_0(1-2t/\tau)\, H(\tau-t) \qquad (2.1)$$

in which comma represents derivative with respect to space and dot, derivative with respect to time. w is the lateral deflection of the plate, and H is the Heaviside function. Defining:

$$\bar{w} = \frac{w}{h}\,, \quad \bar{t} = \frac{t}{\tau_{11}}\,, \quad \bar{t}_o = \frac{t_o}{\tau_{11}}\,, \quad \bar{\tau} = \frac{\tau}{\tau_{11}} = R \qquad (2.2)$$

where τ_{11} is the fundamental period of the plate corresponding to $m = n = 1$ in the following period equation:

$$\tau_{mn} = \frac{2}{\pi}\sqrt{\frac{\mu}{D}}\left[\left(\frac{m}{a}\right)^2 + \left(\frac{n}{b}\right)^2\right]^{-1}, \qquad (2.3)$$

(2.1) may be written as:

$$\frac{d^2\bar{w}}{d\bar{t}^2} + \frac{\tau_{11}^2 D}{\mu}\nabla^4\bar{w} + \frac{\tau_{11}^2}{\mu}\left[Q_0 \sin\frac{2\pi}{\alpha\bar{\tau}}(\bar{t}-\bar{t}_0)H(\bar{t}-\bar{t}_0)H(\alpha\bar{\tau}+\bar{t}_0-\bar{t}) + \tilde{N}_y\right]\bar{w}_{,yy} = \frac{\tau_{11}^2 p_0}{\mu h}(1-2\bar{t}/\bar{\tau})H(\bar{\tau}-\bar{t}). \tag{2.4}$$

The boundary conditions for the plate are:

$$\begin{aligned} \bar{w} &= \bar{w}_{,\bar{x}\bar{x}} = 0 &\quad \text{at } x = 0 \text{ and } x = a, \\ \bar{w} &= \bar{w}_{,\bar{y}\bar{y}} = 0 &\quad \text{at } y = 0 \text{ and } y = b. \end{aligned} \tag{2.5}$$

Letting

$$\bar{w}(x,y,\bar{t}) = \sum_{m=1}^{\infty}\sum_{n=1}^{\infty} T_{mn}(\bar{t})\sin\frac{m\pi x}{a}\sin\frac{n\pi y}{b} \tag{2.6}$$

and expanding the right side of (2.4) in a double sine series, one gets for any (m, n) the following differential equation:

$$\ddot{T}_{mn} + T_{mn}\left\{\left[\left(\frac{2\pi\tau_{11}}{\tau_{mn}}\right)^2 - (2n\pi)^2\frac{\tilde{N}_y}{N_c}\right] - (2n\pi)^2\frac{Q_0}{N_c}\sin\frac{2\pi}{\alpha\bar{\tau}}(\bar{t}-\bar{t}_0)H(\bar{t}-\bar{t}_0)H(\alpha\bar{\tau}+\bar{t}_0-\bar{t})\right\} = \frac{64 p_0 b^2}{mn\pi^2\sigma_c h^2}(1-2\bar{t}/\bar{\tau})H(\bar{\tau}-\bar{t}) \tag{2.7}$$

in which the time derivative is taken with respect to $\bar{t}$ and

$$N_c = h\,\sigma_c$$

$$\sigma_c = \frac{\pi^2 E}{3(1-\nu^2)}\left(\frac{h}{b}\right)^2 \left[\frac{b^2/a^2+1}{2}\right]^2 \quad . \tag{2.8}$$

(2.7) may be written in a simpler form:

$$\ddot{T}_{mn} + T_{mn}\left[B_{mn} - 2S_n \sin\frac{2\pi}{\alpha\bar{\tau}}(\bar{t}-\bar{t}_o)\,H(\bar{t}-\bar{t}_o)\,H(\alpha\bar{\tau}+\bar{t}_o-\bar{t}\,)\right] = f_{mn}\,H(\bar{\tau}-\bar{t}\,) \tag{2.9}$$

with

$$B_{mn} = (2\pi)^2\left[\left(\frac{\tau_{11}}{\tau_{mn}}\right)^2 - \frac{\tilde{N}_Y}{N_c}\,n^2\right]$$

$$2S_n = (2n\pi)^2\,\frac{Q_o}{N_c} \tag{2.10}$$

$$f_{mn} = \frac{64\,p_o}{mn\pi^2\sigma_c}\left(\frac{b}{h}\right)^2 (1-2\bar{t}/\bar{\tau}) \quad .$$

Using the following transformation

$$\eta = \frac{\pi}{\alpha\bar{\tau}}(\bar{t}-\bar{t}_o) - \frac{\pi}{4} \quad , \tag{2.11}$$

(2.9) becomes:

$$\frac{d^2 T_{mn}(\eta)}{d\eta^2} + \left\{A_{mn} - 2q_n\cos 2\eta\; H\!\left[\frac{\alpha\bar{\tau}}{\pi}\left(\eta+\frac{\pi}{4}\right)\right] H\!\left[\alpha\bar{\tau} - \frac{\alpha\bar{\tau}}{\pi}\left(\eta+\frac{\pi}{4}\right)\right]\right\} T_{mn}(\eta) = h_{mn}(\eta)\,H\!\left[\bar{\tau}-\bar{t}_o-\frac{\alpha\bar{\tau}}{\pi}\left(\eta+\frac{\pi}{4}\right)\right] \quad , \tag{2.12}$$

with

$$A_{mn} = 4(\alpha\bar{\tau})^2\left[\left(\frac{\tau_{11}}{\tau_{mn}}\right)^2 - \frac{\tilde{N}_y}{N_c}n^2\right]$$

$$q_n = 2(n\alpha\bar{\tau})^2\frac{Q_0}{N_c} \tag{2.13}$$

$$h_{mn} = \frac{64 p_0 b^2}{mn\sigma_c h^2}\left(\frac{\alpha\bar{\tau}}{\pi^2}\right)^2\left(1 - \frac{2\alpha}{\pi}\left(\eta + \frac{\pi}{4}\right) - 2\frac{\bar{t}_0}{\bar{\tau}}\right) . \tag{2.14}$$

It is assumed that the support at the top of the plate is such that no tensile inplane load is transmitted to the plate. Hence the following condition is specified:

$$\tilde{N}_y - Q_0 \cos 2\eta \geq 0 . \tag{2.15}$$

Three cases for the time-lag are considered: $\bar{t}_o < 0$, $\bar{t}_o = 0$, and $\bar{t}_o > 0$. In the time interval where the inplane pulse is off the plate,(2.12) becomes an ordinary differential equation with constant coefficients, and with proper initial conditions, the solution is easily obtainable. In the time interval where there is an inplane pulse but no lateral load, (2.12) becomes an equation of the Mathieu type. If there is an inplane pulse as well as a lateral load, (2.12) is an inhomogeneous Mathieu equation. The procedure is to solve the Mathieu equation supplemented by the particular solution which may be obtained by the standard method of variation of parameters.

b) Solution to Mathieu's Equation

The following equations are the typical ones that require solution:

$$\ddot{T}(\eta) + (A - 2q\cos 2\eta)\,T(\eta) = h(\eta) \tag{2.16}$$

$$\ddot{T}(\eta) + (A - 2q\cos 2\eta)\,T(\eta) = 0 \tag{2.17}$$

where $\ddot{T}(\eta)$ represents the second derivative of T with respect to η, A and q are given as specified in (2.13). The initial conditions may be specified as follows:

at $\eta = \eta i$ $\qquad T(\eta_i) = D_1$

$$\dot{T}(\eta_i) = D_2$$

where D_1 and D_2 are prescribed or predetermined.

The solution to (2.17) may be written as [8][9]:

$$T = K_1 e^{d\eta} \sum_{s=-\infty}^{\infty} C_{2s} e^{2si} + K_2 e^{-d\eta} \sum_{s=-\infty}^{\infty} C_{2s} e^{-2si} \,, \tag{2.18}$$

where K_1 and K_2 are to be determined by the initial conditions and d is a number, depending on A and q, still to be determined. For the values of A and q chosen in this investigation, the solution, (2.18), would always be stable at large η. Therefore d can be represented by i(β + m), where β is a real fraction and m is an integer. Then for m odd and even (2.18) takes the following forms respectively:

$$T = K_1 \sum_{r=-\infty}^{\infty} C_{2r+1} \cos(2r+1+\beta)\eta + K_2 \sum_{r=-\infty}^{\infty} C_{2r+1} \sin(2r+1+\beta)\eta \tag{2.19a}$$

$$T = K_1 \sum_{r=-\infty}^{\infty} C_{2r} \cos(2r+\beta)\eta + K_2 \sum_{r=-\infty}^{\infty} C_{2r} \sin(2r+\beta)\eta \tag{2.19b}$$

Substituting either term of (2.19a) into (2.17) and setting the coefficient of $\cos(2r+1+\beta)\eta$ or $\sin(2r+1+\beta)\eta$ to zero for $r = -\infty$ to ∞, one obtains the recurrence relation

$$[A - (2r+1+\beta)^2]\, C_{2r+1} - q(C_{2r+3} + C_{2r-1}) = 0. \tag{2.20a}$$

Similarly, using (2.19b) one gets:

$$[A - (2r+\beta)^2]\quad C_{2r} - q(C_{2r+2} + C_{2r-2}) = 0. \tag{2.20b}$$

Allowing r to take both positive and negative integer values as well as zero, a number of simultaneous equations in the same number of unknown coefficients are obtained by truncating (2.20) from both ends. It was found that by truncating the series at $|r| > r_0 = \sqrt{A}/2 + N$ where $N \geq 5$, the terms of the series neglected are very small due to the rapid convergence of the series. Since there are n simultaneous homogeneous equations in n unknown coefficients, the value of β may be determined as an eigenvalue by setting the determinant equal to zero.

This procedure, however, is not suitable because in most cases (except when A is very small) it is very difficult to find β accurately. A more accurate method of obtaining β must be used. This method is discussed in the next section.

The β, evaluated by the method outlined in the next section, is substituted into (2.20), and the coefficients may be determined. An accurate evaluation of the C's depends on the correctness of β used and the procedure by which the C's are determined. If the C's so determined yield a check β which is the same as the original β used, it is an assurance that all the C's are correct. Otherwise, the results are in doubt. Assuming that an accurate β has been obtained, the proper procedure is to set aside the equation having the smallest factor (absolute value) for C_{2r+1} in (2.20a) (or for C_{2r} in (2.20b)). Each coefficient in the remaining equations is then normalized with respect to one of the coefficients, and the equations solved for the normalized coefficients. By using the equation which was singled out at the start, the accuracy of the C's is checked by recovering β and comparing it with the initial value of β. In the present work, the recovered β usually agree with the initial ones to several significant figures.

It is noted that the above procedure is different from that of McLachlan [9] who always sets aside the equation for $r = 0$ in (2.20) for recovering β. When McLachlan's procedure is followed, Table 1 indicates that the check β is far from confirming the fact that the initial β used and therefore the coefficients C determined are correct. It should be pointed out that the initial β listed in Table 1 are obtained by an improved formula supplemented by an iteration procedure. They are believed to be more accurate than those obtained by the existing method [9]. This is confirmed by the fact that by adopting the new procedure outlined above, all the initial β's are confirmed to be almost exact.

Table 1. Comparison of Initial and Check β

A	q	Initial	Check
4.465	0.744	0.0893	0.0570
17.28	2.88	0.1251	0.1803
38.94	0.028	0.2399	6.2250
38.88	6.48	0.18957	0.12413
41.827	.211	0.4674	0.582
69.12	11.525	0.2535	0.371
84.27	14.045	0.11349	0.0572
108.00	18.00	0.31739	1.4828
125.14	15.68	0.155	-0.681
144.00	18.00	0.952	0.679

For modes higher than the fundamental, A is usually very large, and much bigger than q. Then another procedure, namely perturbation, is more efficient for obtaining the solution [9]. Rewrite (2.17) in the following form:

$$\ddot{T} + AT = (2q\cos 2\eta)T \tag{2.21}$$

First neglect the r.h.s., the solution then consists of $\cos\sqrt{A}\,\eta$ and $\sin\sqrt{A}\,\eta$. Now substitute $\cos\sqrt{A}\,\eta$ for T on the r.h.s. of (2.21), there results

$$\ddot{T} + AT = q[\cos(\sqrt{A}+2)\eta + \cos(\sqrt{A}-2)\eta], \tag{2.22}$$

for which the particular solution can be obtained. Substituting the latter for T in (2.21) on the r.h.s., another particular solution may be obtained. By repeating this procedure, and also using $\sin\sqrt{A}\,\eta$, the solution takes the form of an infinite series:

$$T = K_1 \sum_{r=-\infty}^{\infty} C_r \cos(\sqrt{A}-2r)\eta + K_2 \sum_{r=-\infty}^{\infty} C_r \sin(\sqrt{A}-2r)\eta \tag{2.23}$$

with the recurrence relation as follows:

$$4r(\sqrt{A}-r)C_r - q(C_{r-1} + C_{r+1}) = 0.$$

If r << A, the recurrence relation may be simplified to yield:

$$4rC_r - \frac{q}{\sqrt{A}}\left(C_{r-1} + C_{r+1}\right) = 0 \,, \tag{2.24}$$

which is identical to the recurrence relation for the J-Bessel function provided that

$$C_r = J_r(q/2\sqrt{A}) \,. \tag{2.25}$$

When $q/2\sqrt{A} \ll r$, J_r may be represented by the first term of its expansion, or

$$C_r \doteq (q/4\sqrt{A})^r / r! \tag{2.26}$$

giving

$$C_r / C_{r-1} = q/4\sqrt{A}\, r \,.$$

Hence the coefficients decrease very rapidly as r increases. (2.23) may be expressed as:

$$T = K_1 \sum_{r=-r_0}^{r_0} J_r(q/2\sqrt{A}) \cos(\sqrt{A} - 2r)\eta + K_2 \sum_{r=-r_0}^{r_0} J_r(q/2\sqrt{A}) \sin(\sqrt{A} - 2r)\eta \tag{2.27}$$

where r_0 represents the largest r at which the series may be truncated.

Once the solution to (2.17) is available, the solution of (2.16) is obtained by the standard method of variation of parameters taking into consideration the proper initial conditions.

c) Determination of β

Alternatively the solution of (2. 17) may be written after McLachlan [9] as:

$$T = K_1 \, Ce_d(\eta, q) + K_2 \, Se_d(\eta, q) \tag{2.28}$$

where K_1 and K_2 are constants to be determined by the initial conditions and where

$$Ce_d = \cos d\eta + \sum_{r=1}^{\infty} q^r \, \tilde{C}_r(\eta, d) \tag{2.29a}$$

$$Se_d = \sin d\eta + \sum_{r=1}^{\infty} q^r \, \tilde{S}_r(\eta, d) \tag{2.29b}$$

which are known as Mathieu functions of fractional order. The functions, $\tilde{C}_r(\eta, d)$ and $\tilde{S}_r(\eta, d)$ are still to be determined. d is a number which may be represented by $d = m + \beta$ with m an integer and $0 < \beta < 1$.

It is noted from (2. 17) that A and q must be related so that when q vanishes A reduces to d^2 and the solution degenerates to the first terms of (2. 29a) and (2. 29b). Letting

$$A = d^2 + \sum_{r=1}^{\infty} \alpha_r q^r \tag{2.30}$$

and substituting Ce_d and Se_d as T together with (2. 30) into (2.17) and collecting coefficients of like powers of q, there results an infinite number of ordinary differential equations in $\tilde{C}_r$ and $\tilde{S}_r$ which can be solved in sequence. By requiring periodic solutions for $\tilde{C}_r$ and $\tilde{S}_r$, the $\tilde{C}_r$, $\tilde{S}_r$ and α_r can be determined. McLachlan [9] has given the α_r up to α_6. It was found that it does not always yield a sufficiently accurate value of β, and hence the term α_8 is hereby presented. It can be shown that the α_r with odd indices vanish and those with even indices are:

$$\alpha_2 = \frac{1}{2(d^2-1)}$$

$$\alpha_4 = \frac{5d^2+7}{32(d^2-1)^3(d^2-4)}$$

$$\alpha_6 = \frac{9d^4+58d^2+29}{64(d^2-1)^5(d^2-4)(d^2-9)}$$

$$\alpha_8 = \frac{1469d^{10}+9144d^8-14035d^6+64228d^4+827565d^2+274748}{64(128)(d^2-1)^7(d^2-4)^3(d^2-9)(d^2-16)} \quad (2.31)$$

It is seen from (2.30) if $\alpha_2 q^2 << d^2$, and the series is rapidly convergent, as a first approximation $d^2 \doteq A$. Inserting A for d^2 in α_2, and omitting terms of powers of q larger than the second in (2.30), as a second approximation:

$$d^2 = A - \frac{q^2}{2(A-1)} \quad (2.32)$$

Substituting (2.32) for d^2 in α_2, and retaining $d^2 \doteq A$ for the other α_r of (2.31), (2.30) becomes:

$$d^2 = (m+\beta)^2 \doteq \Big[A - \frac{(A-1)q^2}{2(A-1)-q^2} - \frac{(5A+7)q^4}{32(A-1)^3(A-4)}$$

$$- \frac{(9A^2+58A+29)q^6}{64(A-1)^5(A-4)(A-9)}$$

$$- \frac{(1469A^5+9144A^4-14035A^3+64228A^2+827565A+274748)q^8}{64(128)(A-1)^7(A-4)^3(A-9)(A-16)} \Big]. \quad (2.33)$$

Now β may be computed by the following procedure: substituting (2.33) into (2.31) to evaluate the α's which in turn are substituted into (2.30) to compute a new d. The value of d is substituted into (2.31) to determine the new α's which in turn are substituted into (2.30) to compute another d. This procedure is repeated until no substantial change takes place between two iterations. Once d is obtained β can be extracted.

Chapter 3. Response of Rectangular Plates Based on Nonlinear Theory

a) Formulation of Problem

In Chapter 2, the linear behavior of a rectangular plate subjected to the simultaneous application of the disturbances shown in Fig. 1 is studied. However, if the lateral deflection is not small as compared to the thickness of the plate, the linear theory used in Chapter 2 may not give an accurate description of the true behavior of the plate. In essence, the terms that represent the stretching of the middle surface of the plate must be retained resulting in a set of nonlinear equations of motion. The static equivalent is known as the Von Kármán equation [10].

In this chapter, the nonlinear equations of motion will be used to study the same problem dealt with in the previous chapter. The equations and the associated boundary conditions will be derived through the use of Hamilton's Principle in the Appendix. These equations are:

$$
\begin{aligned}
&Dh\left(\frac{\bar{w}_{,\bar{x}\bar{x}\bar{x}\bar{x}}}{a^4} + \frac{2\bar{w}_{,\bar{x}\bar{x}\bar{y}\bar{y}}}{a^2b^2} + \frac{\bar{w}_{,\bar{y}\bar{y}\bar{y}\bar{y}}}{b^4}\right) = \\
&N_x \frac{h}{a^2}\bar{w}_{,\bar{x}\bar{x}} + 2N_{xy}\frac{h}{ab}\bar{w}_{,\bar{x}\bar{y}} + N_y\frac{h}{b^2}\bar{w}_{,\bar{y}\bar{y}} - \frac{\mu h}{\tau_{11}^2}\bar{w}_{,\bar{t}\bar{t}} \\
&+p_0(1-2\bar{t}/\bar{\tau})H(\bar{\tau}-\bar{t}) + \frac{\mu(1-\nu^2)}{E\,\tau_{11}^2}\left(\frac{h}{a}\bar{w}_{,\bar{x}}\bar{u}_{,\bar{t}\bar{t}} + \frac{h}{b}\bar{w}_{,\bar{y}}\bar{v}_{,\bar{t}\bar{t}}\right)
\end{aligned}
\qquad (3.1a)
$$

$$\frac{h}{a^2}\bar{u}_{,\bar{x}\bar{x}} + \frac{(1-\nu)}{2}\frac{h}{b^2}\bar{u}_{,\bar{y}\bar{y}} + \frac{(1+\nu)}{2}\frac{h}{ab}\bar{v}_{,\bar{x}\bar{y}} - \frac{\mu(1-\nu^2)}{E\,\tau_{11}^2}\bar{u}_{,\bar{t}\bar{t}}$$

$$+h^2\left(\frac{\bar{w}_{,\bar{x}}\bar{w}_{,\bar{x}\bar{x}}}{a^3} + \frac{(1-\nu)}{2}\frac{\bar{w}_{,\bar{x}}\bar{w}_{,\bar{y}\bar{y}}}{ab^2} + \frac{(1+\nu)}{2}\frac{\bar{w}_{,\bar{y}}\bar{w}_{,\bar{x}\bar{y}}}{ab^2}\right) = 0 \tag{3.1b}$$

$$\frac{h}{b^2}\bar{v}_{,\bar{y}\bar{y}} + \frac{(1-\nu)}{2}\frac{h}{a^2}\bar{v}_{,\bar{x}\bar{x}} + \frac{(1+\nu)}{2}\frac{h}{ab}\bar{u}_{,\bar{x}\bar{y}} - \frac{\mu(1-\nu^2)}{E\,\tau_{11}^2}\bar{v}_{,\bar{t}\bar{t}}$$

$$+h^2\left(\frac{\bar{w}_{,\bar{y}}\bar{w}_{,\bar{y}\bar{y}}}{b^3} + \frac{(1-\nu)}{2}\frac{\bar{w}_{,\bar{y}}\bar{w}_{,\bar{x}\bar{x}}}{a^2 b} + \frac{(1+\nu)}{2}\frac{\bar{w}_{,\bar{x}}\bar{w}_{,\bar{x}\bar{y}}}{a^2 b}\right) = 0 \tag{3.1c}$$

where $\bar{w} = \frac{w}{h}$, $\bar{u} = \frac{u}{h}$, $\bar{v} = \frac{v}{h}$, $\bar{x} = \frac{x}{a}$, $\bar{y} = \frac{y}{b}$ and $\bar{t} = \frac{t}{\tau_{11}}$.

In addition, the middle surface stresses and strains are:

$$\varepsilon_{xx} = \frac{h}{a}\bar{u}_{,\bar{x}} + \frac{1}{2}\frac{h^2}{a^2}(\bar{w}_{,\bar{x}})^2 \tag{3.2a}$$

$$\varepsilon_{yy} = \frac{h}{b}\bar{v}_{,\bar{y}} + \frac{1}{2}\frac{h^2}{b^2}(\bar{w}_{,\bar{y}})^2 \tag{3.2b}$$

$$\varepsilon_{xy} = \frac{h}{b}\bar{u}_{,\bar{y}} + \frac{h}{a}\bar{v}_{,\bar{x}} + \frac{h^2}{ab}\bar{w}_{,\bar{x}}\bar{w}_{,\bar{y}} \tag{3.2c}$$

$$N_x = \frac{Eh}{(1-\nu^2)}(\varepsilon_{xx} + \nu\,\varepsilon_{yy}) \tag{3.3a}$$

$$N_y = \frac{Eh}{(1-\nu^2)}(\varepsilon_{yy} + \nu\,\varepsilon_{xx}) \tag{3.3b}$$

$$N_{xy} = \frac{Eh}{2(1+\nu)} \varepsilon_{xy} \tag{3.3c}$$

The plate is simply supported in the lateral direction. In the plane of the plate the edge $\bar{y} = 0$ is restrained from motion and the vertical edges are either allowed to move or be restricted from motion. All the edges are restricted to remain straight. At the top $(\bar{y} = 1)$, the straight edge condition is maintained by having a rigid bar. The rigid bar may be massless or may have a distributed mass. Therefore the boundary conditions can be stated as:

$$\bar{w} = \bar{w}_{,\bar{x}\bar{x}} = 0 \qquad \text{at } \bar{x} = 0 \text{ and } \bar{x} = 1$$

$$\bar{w} = \bar{w}_{,\bar{y}\bar{y}} = 0 \qquad \text{at } \bar{y} = 0 \text{ and } \bar{y} = 1 \tag{3.4a}$$

$$\bar{u} = \varphi_x(\bar{t}) \qquad \text{at } \bar{x} = 0$$

$$\bar{u} = -\varphi_x(\bar{t}) \qquad \text{at } \bar{x} = 1$$

$$\bar{v} = 0 \qquad \text{at } \bar{y} = 0$$

$$\bar{v} = \varphi_y(\bar{t}) \qquad \text{at } \bar{y} = 1 \tag{3.4b}$$

$$N_{xy} = 0 \qquad \text{at } \bar{x} = 0,\ \bar{x} = 1,\ \bar{y} = 0, \text{ and } \bar{y} = 1 \tag{3.4c}$$

It is noted that when the vertical sides are restrained from motion, $\varphi_x(\bar{t})$ is zero at $\bar{x} = 0$ and $\bar{x} = 1$.

b) Solution for a Rectangular Plate with Movable Vertical Sides

Let the solution for $\bar{w}$ be:

$$\bar{w}(\bar{x}, \bar{y}, \bar{t}) = A(\bar{t}) \sin \pi \bar{x} \sin \pi \bar{y} + B(\bar{t}) \sin \pi \bar{x} \sin 3\pi \bar{y} + C(\bar{t}) \sin 3\pi \bar{x} \sin \pi \bar{y} \tag{3.5}$$

where $A(\bar{t})$, $B(\bar{t})$ and $C(\bar{t})$ are functions of time. Substituting into (3.1b) and (3.1c) and retaining the products of A^2, AB and AC, the two coupled partial differential equations become:

$$\frac{h}{a^2} \bar{u}_{,\bar{x}\bar{x}} + \frac{(1-\nu)}{2} \frac{h}{b^2} \bar{u}_{,\bar{y}\bar{y}} + \frac{(1+\nu)}{2} \frac{h}{ab} \bar{v}_{,\bar{x}\bar{y}} - \frac{\mu(1-\nu^2)}{E \tau_{11}^2} \bar{u}_{,\bar{t}\bar{t}} + \xi_1 = 0 \tag{3.6}$$

$$\frac{h}{b^2} \bar{v}_{,\bar{y}\bar{y}} + \frac{(1-\nu)}{2} \frac{h}{a^2} \bar{v}_{,\bar{x}\bar{x}} + \frac{(1+\nu)}{2} \frac{h}{ab} \bar{u}_{,\bar{x}\bar{y}} - \frac{\mu(1-\nu^2)}{E \tau_{11}^2} \bar{v}_{,\bar{t}\bar{t}} + \xi_2 = 0 \tag{3.7}$$

where

$$\begin{aligned}\xi_1(\bar{x}, \bar{y}, \bar{t}) = \frac{\pi^3 h^2}{4a^3 b^2} \Big\{ & A^2 \left[(-b^2 + \nu a^2) \sin 2\pi\bar{x} + (b^2 + a^2) \sin 2\pi\bar{x} \cos 2\pi\bar{y} \right] \\ & + AB \left[(-2b^2 + (-2+8\nu)a^2) \sin 2\pi\bar{x} \cos 2\pi\bar{y} \right. \\ & \quad \left. + (2b^2 + (8-2\nu)a^2) \sin 2\pi\bar{x} \cos 4\pi\bar{y} \right] \\ & + AC \left[(-6b^2 - 2\nu a^2) \sin 2\pi\bar{x} + (-12b^2 + 4\nu a^2) \sin 4\pi\bar{x} \right. \\ & \quad + (6b^2 - 2a^2) \sin 2\pi\bar{x} \cos 2\pi\bar{y} \\ & \quad \left. + (12b^2 + 4a^2) \sin 4\pi\bar{x} \cos 2\pi\bar{y} \right] \Big\}\end{aligned}$$

and

$$\xi_2(\bar{x},\bar{y},\bar{t}) = \frac{\pi^3 h^2}{4a^2 b^3} \Big\{ A^2 \left[(-a^2+\nu b^2)\sin 2\pi\bar{y} + (a^2+b^2)\sin 2\pi\bar{y}\cos 2\pi\bar{x} \right]$$
$$+ AB\left[(-6a^2 - 2\nu b^2)\sin 2\pi\bar{y} + (-12a^2 + 4\nu b^2)\sin 4\pi\bar{y} \right.$$
$$+ (6a^2 - 2b^2)\sin 2\pi\bar{y}\cos 2\pi\bar{x}$$
$$\left. + (12a^2 + 4b^2)\sin 4\pi\bar{y}\cos 2\pi\bar{x} \right]$$
$$+ AC\left[(-2a^2 + (-2+8\nu)b^2)\sin 2\pi\bar{y}\cos 2\pi\bar{x} \right.$$
$$\left. + (2a^2 + (8-2\nu)b^2)\sin 2\pi\bar{y}\cos 4\pi\bar{x} \right] \Big\}$$

Solutionsfor $\bar{u}(\bar{x}, \bar{y}, \bar{t})$ and $\bar{v}(\bar{x}, \bar{y}, \bar{t})$

Let

$$\bar{u}(\bar{x}, \bar{y}, \bar{t}) = \bar{u}_1(\bar{x}, \bar{y}, \bar{t}) + \bar{u}_2(\bar{x}, \bar{y}, \bar{t}) \tag{3.8a}$$

and

$$\bar{v}(\bar{x}, \bar{y}, \bar{t}) = \bar{v}_1(\bar{x}, \bar{y}, \bar{t}) + \bar{v}_2(\bar{x}, \bar{y}, \bar{t}) \tag{3.8b}$$

where $\bar{u}_1(\bar{x}, \bar{y}, \bar{t})$ and $\bar{v}_1(\bar{x}, \bar{y}, \bar{t})$ satisfy the homogeneous differential equations $(\xi_1 = \xi_2 = 0)$ with the inhomogeneous boundary conditions (i.e., (3.4b) and (3.4c)) and $\bar{u}_2(\bar{x}, \bar{y}, \bar{t})$ and $\bar{v}_2(\bar{x}, \bar{y}, \bar{t})$ satisfy equations (3.6) and (3.7) with homogeneous boundary conditions (i.e., (3.4b) and (3.4c) with $\varphi_x = \varphi_y = 0$).

Displacements $\bar{u}_2(\bar{x}, \bar{y}, \bar{t})$ and $\bar{v}_2(\bar{x}, \bar{y}, \bar{t})$

Let

$$
\begin{aligned}
\bar{u}_2(\bar{x},\bar{y},\bar{t}) = {} & \bar{u}^{20AA} \sin 2\pi\bar{x} + \bar{u}^{22AA} \sin 2\pi\bar{x}\cos 2\pi\bar{y} \\
& + \bar{u}^{22AB} \sin 2\pi\bar{x}\cos 2\pi\bar{y} + \bar{u}^{24AB}\sin 2\pi\bar{x}\cos 4\pi\bar{y} \\
& + \bar{u}^{20AC} \sin 2\pi\bar{x} + \bar{u}^{40AC}\sin 4\pi\bar{x} \\
& + \bar{u}^{22AC} \sin 2\pi\bar{x}\cos 2\pi\bar{y} + \bar{u}^{42AC}\sin 4\pi\bar{x}\cos 2\pi\bar{y}
\end{aligned} \tag{3.9a}
$$

and

$$
\begin{aligned}
\bar{v}_2(\bar{x},\bar{y},\bar{t}) = {} & \bar{v}^{02AA} \sin 2\pi\bar{y} + \bar{v}^{22AA} \cos 2\pi\bar{x}\sin 2\pi\bar{y} \\
& + \bar{v}^{02AB} \sin 2\pi\bar{y} + \bar{v}^{04AB}\sin 4\pi\bar{y} \\
& + \bar{v}^{22AB} \cos 2\pi\bar{x}\sin 2\pi\bar{y} + \bar{v}^{24AB}\cos 2\pi\bar{x}\sin 4\pi\bar{y} \\
& + \bar{v}^{22AC} \cos 2\pi\bar{x}\sin 2\pi\bar{y} + \bar{v}^{42AE}\cos 4\pi\bar{x}\sin 2\pi\bar{y} \, .
\end{aligned} \tag{3.9b}
$$

The superscripts of $\bar{u}$ and $\bar{v}$ are used for easy identification of the terms.

The analysis is greatly simplified if the longitudinal inertia terms in (3.6) and (3.7) are neglected. To compensate for the effect of longitudinal inertia, it is assumed that all the mass of the plate is concentrated at the top of the plate along a rigid bar.

Substituting (3. 9a) and (3. 9b) into (3. 6) and (3. 7) and comparing the coefficients of each $\sin m\pi\bar{x}\cos n\pi\bar{y}$ (Equation (3. 6)) and $\cos p\pi\bar{x}\sin r\pi\bar{y}$ (Equation (3. 7)), the unknown coefficients in (3. 9a) and (3. 9b) can be determined in terms of the unknown time functions of the lateral displacements. This results in the following expressions for $\bar{u}_2$ and $\bar{v}_2$:

$$\bar{u}_2(\bar{x},\bar{y},\bar{t}) = \pi h \Big\{ A^2 \left[\frac{(-b^2+\nu a^2)\sin 2\pi\bar{x}}{16ab^2} + \frac{1}{16a}\sin 2\pi\bar{x}\cos 2\pi\bar{y}\right]$$

$$+AB\left[\frac{(a^2b^2(-2+4\nu)-b^4-5a^4)}{8a(a^2+b^2)^2}\sin 2\pi\bar{x}\cos 2\pi\bar{y}\right.$$

$$\left.+\frac{(a^2b^2(8-\nu)+b^4+20a^4)}{8a(4a^2+b^2)^2}\sin 2\pi\bar{x}\cos 4\pi\bar{y}\right]$$

$$+AC\left[\frac{(-6b^2-2\nu a^2)\sin 2\pi\bar{x}}{16ab^2}+\frac{(-12b^2+4\nu a^2)\sin 4\pi\bar{x}}{64ab^2}\right.$$

$$+\frac{(a^2b^2(6+4\nu)+3b^4-a^4)}{8a(a^2+b^2)^2}\sin 2\pi\bar{x}\cos 2\pi\bar{y}$$

$$\left.+\frac{(a^2b^2(6-\nu)+12b^4+a^4)}{4a(a^2+4b^2)^2}\sin 4\pi\bar{x}\cos 2\pi\bar{y}\right]\Big\} \tag{3.10a}$$

and

$$\bar{v}_2(\bar{x},\bar{y},\bar{t}) = \pi h \Big\{ A^2 \left[\frac{(-a^2+\nu b^2)}{16ba^2} \sin 2\pi\bar{y} \quad + \frac{1}{16b} \cos 2\pi\bar{x} \sin 2\pi\bar{y} \right]$$

$$+AB\left[\frac{(-6a^2-2\nu b^2)}{16ba^2} \sin 2\pi\bar{y} + \frac{(-12a^2+4\nu b^2)}{64ba^2} \sin 4\pi\bar{y} \right.$$

$$+ \frac{(a^2b^2(6+4\nu)+3a^4-b^4)}{8b(a^2+b^2)^2} \cos 2\pi\bar{x} \sin 2\pi\bar{y}$$

$$\left. + \frac{(a^2b^2(6-\nu)+12a^4+b^4)}{4b(4a^2+b^2)^2} \cos 2\pi\bar{x} \sin 4\pi\bar{y} \right]$$

$$+AC\left[\frac{(a^2b^2(-2+4\nu)-a^4-5b^4)}{8b(a^2+b^2)^2} \cos 2\pi\bar{x} \sin 2\pi\bar{y} \right.$$

$$\left. + \frac{(a^2b^2(8-\nu)+a^4+20b^4)}{8b(a^2+4b^2)^2} \cos 4\pi\bar{x} \sin 2\pi\bar{y} \right] \Big\} \,. \tag{3.10b}$$

Displacements $\bar{u}_1(\bar{x},\bar{y},\bar{t})$ and $\bar{v}_1(\bar{x},\bar{y},\bar{t})$

Letting

$$\bar{u}_1(\bar{x},\bar{y},\bar{t}) = (1-2\bar{x})\,\varphi_x(\bar{t}) \tag{3.11a}$$

$$v_1(\bar{x},\bar{y},\bar{t}) = -\bar{y}\,\varphi_y(\bar{t}) \quad , \tag{3.11b}$$

it is seen that the boundary conditions and the homogeneous equations of motion are identically satisfied. The functions $\varphi_x(\bar{t})$ and $\varphi_y(\bar{t})$ are obviously related, and may be determined by the equilibrium conditions along the boundaries.

First consider the dynamic equilibrium of the rigid loading bar:

$$\int_0^1 N_y(\bar{x}, 1, \bar{t})\, d\bar{x} = -\left(\tilde{N}_y + Q_0 \sin\frac{2\pi\bar{t}}{\alpha\bar{\tau}} H(\alpha\bar{\tau} - \bar{t}) - \frac{M_b h}{\tau_{11}^2} \frac{d^2\varphi_y}{d\bar{t}^2}\right). \tag{3.12}$$

Using (3.2) and (3.3), (3.12) becomes:

$$\frac{d^2\varphi_y}{d\bar{t}^2} + \tau_{11}^2 \omega_0^2 \left(\varphi_y + 2\nu \frac{b}{a} \varphi_x\right) = \frac{\tau_{11}^2}{M_b h}\left(\tilde{N}_y + Q_0 \sin\frac{2\pi\bar{t}}{\alpha\bar{\tau}} H(\alpha\bar{\tau} - \bar{t})\right)$$

$$+ \tau_{11}^2 \omega_0^2 \pi^2 \frac{h}{b} \frac{A^2}{8}\left(1 + \nu \frac{b^2}{a^2}\right) \tag{3.12a}$$

where $\omega_0^2 = \dfrac{Eh}{M_b b(1-\nu^2)}$ and M_b is the mass per unit length of the rigid bar. Since the vertical sides are movable, the stress resultants along the boundaries $\bar{x} = 0$ and $\bar{x} = 1$ should vanish, which gives:

$$2\frac{b}{a} \varphi_x(\bar{t}) = \frac{\pi^2 bh}{a^2} \frac{A^2}{8}\left(1 + \nu \frac{a^2}{b^2}\right) - \nu \varphi_y(\bar{t}) \quad . \tag{3.13}$$

Substituting (3.13) into (3.12) yields:

$$\frac{d^2\varphi_y}{d\bar{t}^2} + (\tau_{11}\omega_0)^2 (1-\nu^2)\varphi_y = \frac{\tau_{11}^2}{M_b h}\left(\tilde{N}_y + Q_0 \sin\frac{2\pi\bar{t}}{\alpha\bar{\tau}} H(\alpha\bar{\tau} - \bar{t})\right)$$

$$+ (\tau_{11}\omega_0)^2 \frac{\pi^2 h}{b} \frac{A^2}{8} (1-\nu^2) \quad . \tag{3.14}$$

Lateral Displacement

Substituting (3. 10) and (3. 11) into (3. 8) to get $\bar{u}$ and $\bar{v}$, and in turn $\bar{u}$, $\bar{v}$ and $\bar{w}$, (3. 5), into (3. 2), (3. 3) and (3. 1a), the last equation, (3. 1a), governing the lateral displacement can be reduced to three ordinary nonlinear coupled differential equations by using the Galerkin method [12]. These equations are:

$$\frac{d^2A}{d\bar{t}^2} + \frac{D\pi^4\tau_{11}^2}{\mu}\left(\frac{1}{a^2}+\frac{1}{b^2}\right)^2 A = \frac{16\,\tau_{11}^2\,p_0}{\mu\, h\,\pi^2}\,(1-2\bar{t}/\bar{\tau})\,H(\bar{\tau}-\bar{t})$$

$$-\frac{Eh^3\pi^4\tau_{11}^2}{16\mu}\left\{\frac{A^3}{(1-\nu^2)}\left(\frac{3-\nu^2}{a^4}+\frac{4\nu}{a^2b^2}+\frac{3-\nu^2}{b^4}\right)-\frac{3A^2B}{a^4}-\frac{3A^2C}{b^4}\right.$$

$$\left.-\frac{16A}{\pi^2h(1-\nu^2)}\left[\varphi_y\left(\frac{\nu}{a^2b}+\frac{1}{b^3}\right)+2\varphi_x\left(\frac{1}{a^3}+\frac{\nu}{ab^2}\right)\right]\right\} \qquad (3.\ 15)$$

$$\frac{d^2B}{d\bar{t}^2} + \frac{D\pi^4\tau_{11}^2}{\mu}\left(\frac{1}{a^2}+\frac{9}{b^2}\right)^2 B = \frac{16\,\tau_{11}^2\,p_0}{3\mu\, h\,\pi^2}\,(1-2\bar{t}/\bar{\tau})\,H(\bar{\tau}-\bar{t})$$

$$-\frac{Eh^3\pi^4\tau_{11}^2}{16\mu}\left\{\frac{A^2B}{(1-\nu^2)}\left(\frac{6-9\nu^2}{a^4}+\frac{20\nu}{a^2b^2}+\frac{27-9\nu^2}{b^4}\right)-\frac{A^3}{a^4}+\frac{A^2B}{(9a^2+b^2)^2}\right. \qquad (3.\ 16)$$

$$\left.+\frac{16A^2C}{(a^2+b^2)^2}+\frac{16A^2B}{(a^2+b^2)^2}-\frac{16B}{\pi^2h(1-\nu^2)}\left[\varphi_y\left(\frac{\nu}{a^2b}+\frac{9}{b^3}\right)+2\varphi_x\left(\frac{1}{a^3}+\frac{9\nu}{ab^2}\right)\right]\right\}$$

$$\frac{d^2C}{d\bar{t}^2} + \frac{D\pi^4\tau_{11}^2}{\mu}\left(\frac{9}{a^2}+\frac{1}{b^2}\right)^2 C = \frac{16\,\tau_{11}\,p_o}{3\mu h\pi^2}\,(1-2\bar{t}/\bar{\tau})\,H(\bar{\tau}-\bar{t})$$

$$-\frac{Eh^3\pi^4\tau_{11}^2}{16\mu}\left\{\frac{A^2C}{1-\nu^2}\left(\frac{27-9\nu^2}{a^4}+\frac{20\nu}{a^2b^2}+\frac{6-9\nu^2}{b^4}\right)-\frac{A^3}{b^4}+\frac{A^2C}{(a^2+4b^2)^2}\right. \qquad (3.17)$$

$$\left.+\frac{16A^2C}{(a^2+b^2)^2}+\frac{16A^2B}{(a^2+b^2)^2}-\frac{16C}{\pi^2h(1-\nu^2)}\left[\varphi_y\left(\frac{9\nu}{a^2b}+\frac{1}{b^3}\right)+2\varphi_x\left(\frac{9}{a^3}+\frac{\nu}{ab^2}\right)\right]\right\}$$

To simplify the present analysis a square plate is now considered. Eliminating φ_x from (3.15), (3.16) and (3.17), one gets:

$$\frac{d^2A}{d\bar{t}^2} + 4\pi^2 A = \frac{192\,p_o(1-\nu^2)}{\pi^4 E}\left(\frac{a}{h}\right)^4(1-2\bar{t}/\bar{\tau})\,H(\bar{\tau}-\bar{t})$$

$$-\frac{3\pi^2(1-\nu^2)}{4}\left[4A^3-3A^2B-3A^2C-\frac{16A\varphi_y}{\pi^2}\,\frac{a}{h}\right] \qquad (3.18)$$

$$\frac{d^2B}{d\bar{t}^2} + 100\pi^2 B = \frac{64\,p_o(1-\nu^2)}{\pi^4 E}\left(\frac{a}{h}\right)^4(1-2\bar{t}/\bar{\tau})\,H(\bar{\tau}-\bar{t})$$

$$-\frac{3\pi^2(1-\nu^2)}{4}\left[A^2B\left(35+\frac{1}{25}\right)-A^3+4A^2C-\frac{144B\varphi_y}{\pi^2}\,\frac{a}{h}\right] \qquad (3.19)$$

$$\frac{d^2C}{d\bar{t}^2} + 100\pi^2 C = \frac{64\,p_o(1-\nu^2)}{\pi^4 E}\left(\frac{a}{h}\right)^4(1-2\bar{t}/\bar{\tau})\,H(\bar{\tau}-\bar{t})$$

$$-\frac{3\pi^2(1-\nu^2)}{4}\left[A^2C\left(19+\frac{1}{25}\right)-A^3+4A^2B-\frac{16C\varphi_y}{\pi^2}\,\frac{a}{h}\right] \qquad (3.20)$$

$$\frac{d^2\varphi_y}{d\bar{t}^2} + \frac{12a^2(1-\nu^2)}{\pi^2 h^2 k}\varphi_y = \frac{4a}{hk}\left(\frac{N_y}{N_0} + \frac{N_1}{N_0}\sin\frac{[illegible]}{[illegible]}H(\alpha\bar{t}-\bar{t})\right) \tag{3.21}$$

$$+ \frac{3a(1-\nu^2)}{2hk}A^2$$

where [illegible] $= \frac{N_t}{[illegible]}$, [illegible] and [illegible] $= \frac{[illegible]}{a^2}$ [illegible].

It is noted that if only the force [illegible] along the boundary [illegible] is considered instead of a rigid loading [illegible] distributed mass an explicit expression between φ_y and A can be found immediately from (3.21):

$$(1-\nu^2)\varphi_y = \frac{\pi^2 h}{3a}\left[\frac{N_y}{N_0} + \frac{N_1}{N_0}\sin\frac{[illegible]}{[illegible]}H(\alpha\bar{t}-t)\right] + [illegible]\frac{A^2}{ab}[illegible] \tag{3.22}$$

It is believed that the effect of the longitudinal inertia should be bounded by the following two cases: one with the mass of the plate concentrated in a rigid bar and the other with the mass neglected. It will be shown in the next chapter that with $\frac{N}{N_0}$ [illegible], the response of the plate is approximately the same for both cases.

c) Solution for a Rectangular Plate with Immovable Vertical Sides

If the vertical sides of the plate are immovably constrained at $\bar{x} = 0$ and $\bar{x} = 1$ $(\bar{u} = 0)$, the displacement $\bar{u}_1 = 0$ will satisfy the homogeneous part of (3. 6) and (3. 7) and the boundary conditions. Then with $\varphi_x = 0$, (3. 14) becomes:

$$\frac{d^2\varphi_y}{d\bar{t}^2} + (\tau_{11}\omega_0)^2\varphi_y = \frac{\tau_{11}^2}{M_b h}\left(\tilde{N}_y + Q_0 \sin\frac{2\pi\bar{t}}{\alpha\bar{\tau}} H(\alpha\bar{\tau} - \bar{t})\right)$$

$$+ (\tau_{11}\omega_0)^2 \pi^2 \frac{h}{b}\frac{A^2}{8}\left(1 + \nu\frac{b^2}{a^2}\right). \tag{3. 14a}$$

The equations governing the lateral deflection((3. 15), (3. 16), and (3. 17)) become:

$$\frac{d^2A}{d\bar{t}^2} + \frac{D\pi^4\tau_{11}^2}{\mu}\left(\frac{1}{a^2} + \frac{1}{b^2}\right)^2 A = \frac{16\,\tau_{11}^2 p_0}{\mu h \pi^2}(1 - 2\bar{t}/\bar{\tau})H(\bar{\tau} - \bar{t})$$

$$- \frac{Eh^3\pi^4\tau_{11}^2}{16\mu}\left\{\frac{A^3}{1-\nu^2}\left(\frac{3-\nu^2}{a^4} + \frac{4\nu}{a^2b^2} + \frac{3-\nu^2}{b^4}\right) - \frac{3A^2B}{a^4} - \frac{3A^2C}{b^4}\right.$$

$$\left. - \frac{16A\varphi_y}{\pi^2 h(1-\nu^2)}\left(\frac{\nu}{a^2 b} + \frac{1}{b^3}\right)\right\} \tag{3. 15a}$$

$$\frac{d^2B}{d\bar{t}^2} + \frac{D\pi^4\tau_{11}^2}{\mu}\left(\frac{1}{a^2} + \frac{9}{b^2}\right)B = \frac{16\,\tau_{11}^2 p_0}{3\mu h\pi^2}(1 - 2\bar{t}/\bar{\tau})H(\bar{\tau} - \bar{t})$$

$$- \frac{Eh^3\pi^4\tau_{11}^2}{16\mu}\left\{\frac{A^2B}{1-\nu^2}\left(\frac{6-4\nu^2}{a^4} + \frac{20\nu}{a^2b^2} + \frac{27-9\nu^2}{b^4}\right) - \frac{A^3}{a^4} + \frac{A^2B}{(4a^2+b^2)^2}\right.$$

$$\left. + \frac{16A^2C}{(a^2+b^2)^2} + \frac{16A^2B}{(a^2+b^2)^2} - \frac{16B\varphi_y}{\pi^2 h(1-\nu^2)}\left(\frac{\nu}{a^2 b} + \frac{9}{b^3}\right)\right\} \tag{3. 16a}$$

$$\frac{d^2C}{d\bar{t}^2} + \frac{D\pi^4\tau_{11}^2}{\mu}\left(\frac{9}{a^2}+\frac{1}{b^2}\right)^2 C = \frac{16\,\tau_{11}\,p_o}{3\mu h\pi^2}\,(1-2\bar{t}/\bar{\tau})\,H(\bar{\tau}-\bar{t})$$

$$-\frac{Eh^3\pi^4\tau_{11}^2}{16\mu}\left\{\frac{A^2C}{1-\nu^2}\left(\frac{27-9\nu^2}{a^4}+\frac{20\nu}{a^2b^2}+\frac{6-4\nu^2}{b^4}\right)-\frac{A^3}{b^4}+\frac{A^2C}{(a^2+4b^2)^2}\right. \qquad (3.17a)$$

$$\left.+\frac{16A^2B}{(a^2+b^2)^2}+\frac{16A^2C}{(a^2+b^2)^2}-\frac{16C\varphi_y}{\pi^2h(1-\nu^2)}\left(\frac{9\nu}{a^2b}+\frac{1}{b^3}\right)\right\} .$$

For a square plate of sides, a, (3.18) - (3.21) become:

$$\frac{d^2A}{d\bar{t}^2} + 4\pi^2 A = \frac{192\,p_o(1-\nu^2)}{\pi^4 E}\left(\frac{a}{h}\right)^4(1-2\bar{t}/\bar{\tau})\,H(\bar{\tau}-\bar{t})$$

$$-\frac{3\pi^2(1-\nu^2)}{4}\left\{\frac{A^3}{1-\nu^2}(6+4\nu-2\nu^2)-3A^2B-3A^2C-\frac{16A\varphi_y a(1+\nu)}{\pi^2(1-\nu^2)h}\right\} \qquad (3.18a)$$

$$\frac{d^2B}{d\bar{t}^2} + 100\pi^2 B = \frac{64\,p_o(1-\nu^2)}{\pi^4 E}\left(\frac{a}{h}\right)^4(1-2\bar{t}/\bar{\tau})\,H(\bar{\tau}-\bar{t}) - \frac{3\pi^2(1-\nu^2)}{4}$$

$$\left\{\frac{A^2B}{1-\nu^2}\left(33+20\nu-13\nu^2+\left(4+\frac{1}{25}\right)(1-\nu^2)\right)-A^3+4A^2C\;-\frac{16B\varphi_y a(9+\nu)}{\pi^2(1-\nu^2)h}\right\} \qquad (3.19a)$$

$$\frac{d^2C}{d\bar{t}^2} + 100\pi^2 C = \frac{64\,p_o(1-\nu^2)}{\pi^4 E}\left(\frac{a}{h}\right)^4(1-2\bar{t}/\bar{\tau})\,H(\bar{\tau}-\bar{t}) - \frac{3\pi^2(1-\nu^2)}{4}$$

$$\left\{\frac{A^2C}{1-\nu^2}\left(33+20\nu-13\nu^2+\left(4+\frac{1}{25}\right)(1-\nu^2)\right)-A^3+4A^2B\;-\frac{16C\varphi_y a(9\nu+1)}{\pi^2(1-\nu^2)h}\right\} \qquad (3.20a)$$

$$\frac{d^2\varphi_Y}{d\bar{t}^2} + \frac{12a^2}{\pi^2 k h^2}\varphi_Y = \frac{4a}{kh}\left(\frac{\tilde{N}_Y}{N_c} + \frac{Q_c}{N_c}\sin\frac{2\pi\bar{t}}{\alpha\bar{\tau}} H(\alpha\bar{\tau}-\bar{t})\right)$$

$$+ \frac{3a(1+\nu)}{2kh} A^2 . \qquad (3.21a)$$

Neglecting the inertia of the rigid bar, (3.21a) becomes:

$$\varphi_Y = \frac{\pi^2 h}{3a}\left(\frac{\tilde{N}_Y}{N_c} + \frac{Q_0}{N_c}\sin\frac{2\pi\bar{t}}{\alpha\bar{\tau}} H(\alpha\bar{\tau}-\bar{t})\right) + \frac{\pi^2 h}{a}\frac{A^2}{8}(1+\nu) . \qquad (3.22a)$$

d) Numerical Procedure

The system of nonlinear ordinary differential equations ((3.18) - (3.21) and(3.18a) - (3.21a)) was solved on the IBM 360-50 computer at The City College of New York using Hamming's modified predictor-corrector integration scheme [15]. It involves computations of certain items as given below:

Predictor: $p_{n+1} = y_{n-3} + \frac{4\Delta t}{3}\left(2y'_n - y'_{n-1} + 2y'_{n-2}\right)$

Modifier: $m_{n+1} = p_{n+1} - \frac{112}{121}(p_n - c_n)$

$m'_{n+1} = f(t_{n+1}, m+1)$

Corrector: $c_{n+1} = \frac{1}{8}\left[9y_n - y_{n-2} + 3h(m'_{n+1} + 2y'_n - y'_{n-1})\right]$

Final Value: $y_{n+1} = c_{n+1} + \frac{9}{121}(p_{n+1} - c_{n+1})$

This scheme is a stable fourth-order integration procedure that requires the evaluation of the right hand side of a system of differential equations of the form $y' = f(t, y)$ only two times per step. It also has the advantage of being able to estimate the local truncation error at each step and thus the procedure is able to choose and change the step size without a significant amount of computation time.

Since this scheme is not self starting, a Runga-Kutta method, which only requires the initial conditions to begin the solution, is used to start the solution. Since the Runga-Kutta method is used only for starting the solution, matters such as stability and minimization of roundoff errors are not important. The only criterion of significance is minimization of the truncation error. According to Ralston [16], the Runga-Kutta scheme which has the most favorable bound of the truncation error is:

$$y_{n+1} = y_n + .17476028\, k_1 - .55148066\, k_2 + 1.20553560\, k_3 + .17118478\, k_4$$

where

$$k_1 = \Delta t_n\, f(t_n, y_n)$$
$$k_2 = \Delta t_n\, f(t_n + .4\Delta t_n, y_n + .4k_1)$$
$$k_3 = \Delta t_n\, f(t_n + .45573725\,\Delta t_n, y_n + .29697761\, k_1 + .15875964\, k_2)$$
$$k_4 = \Delta t_n\, f(t_n + \Delta t_n, y_n + .21810040\, k_1 - 3.05096516\, k_2 + 3.83286476\, k_3).$$

Since it is very important that these starting values be as accurate as possible, they are refined by one iteration step using the following fourth-order interpolation formula:

$$y_1 = y_0 + \frac{\Delta t_n}{24}(9y_0' + 19y_1' - 5y_2' + y_3')$$

$$y_2 = y_0 + \frac{\Delta t_n}{3}(y_0' + 4y_1' + y_2')$$

$$y_3 = y_0 + \frac{3\Delta t_n}{8}(y_0' + 3y_1' + 3y_2' + y_3') .$$

Chapter 4. Dynamic Response of a Square Plate

The solutions presented in Chapter 2 based on the linear theory and in Chapter 3 based on the nonlinear theory are now applied to a square plate. After the time functions are determined, the bending stresses and the membrane stresses can be determined. Since one is concerned with the maximum stress, the severity of the dynamic response of the plate to the dynamic loadings can be conveniently displayed by a dimensionless quantity known as the dynamic amplification factor for stress (hereafter DAF). In what follows, the DAF will be first defined and then followed by a presentation of the results obtained by the linear and nonlinear theories. A comparison of the results will be made which serves to delineate the limit of validity of the linear model.

a) Dynamic Amplification Factor

The DAF is defined as the ratio of the maximum dynamic stress to the maximum static stress or

$$DAF = (\sigma_d + \sigma_y)/\sigma_s \tag{4.1}$$

where σ_d is the dynamic bending stress at the center of the plate given by [14]:

$$\sigma_d = \frac{6D}{a^2 h}\left(\bar{w}_{,\bar{y}\bar{y}} + \nu \bar{w}_{,\bar{x}\bar{x}}\right) \tag{4.2}$$

and σ_y, the inplane stress which is the sum of the inplane prestress, $\tilde{N}_y/h$, and the dynamic inplane stress, Q_c/h, which occurs at the same time as the dynamic bending stress, σ_d. The static stress, σ_s, is the bending stress at the center of a square plate of sides, a, and thickness, h, subjected to a uniform pressure p_o. It is noted that σ_s is a fictitious stress used for convenience. Assuming ν to be 0.231 [17] σ_s can be computed by:

$$\sigma_s = 0.271\, p_o\, (a/h)^2 \tag{4.3}$$

If the DAF is known for a given plate subjected to a given disturbance, the maximum dynamic stress can be easily obtained. Further when one compares the DAF's obtained from the linear and nonlinear models, one is essentially comparing the maximum stress amplitudes evaluated by the respective models.

b) Response of Plate Based on Linear Theory

The dynamic response of the plate subjected to a simultaneous lateral N-shaped pressure pulse and a sinusoidal inplane pulse is now considered using the linear theory. The case with no time-lag is considered first, followed by the case with either a positive or negative time-lag. A positive time-lag means that the lateral disturbance leads the inplane disturbance by a certain time and a negative time-lag, the inplane disturbance leads the lateral disturbance by a certain time.

Due to the large number of parameters involved, it would be impractical to try to locate the absolute maximum DAF by varying all the parameters. On the other hand, it is now possible to investigate a few typical cases so as to learn the trend and the order of magnitude by which the interaction of the various parameters can be better understood. In all cases the ratio, a/h, was taken to be 240[17] which corresponds to what is being used for relatively large glass panes installed commercially.

In evaluating the time functions, the first nine symmetric modes are computed and the contribution of higher modes are neglected. Due to the rapid convergence of the series solution, reliable results can be obtained by considering just the first three modes as demonstrated in Table 2 for a typical case.

Table 2. Comparison of Maximum Response - Three Versus Nine Modes

$p_o = 2$ $\tilde{N}_y / N_c = 0$ $Q_o / N_c = 1/4$

R	Three Modes		Nine Modes	
	$\overline{w}$	DAF	$\overline{w}$	DAF
.60	0.422	2.190	0.424	2.270
.80	0.559	2.821	0.560	2.881
.95	0.581	2.830	0.581	2.869
1.20	0.512	2.565	0.512	2.644
1.40	0.453	2.568	0.454	2.633
1.60	0.438	2.763	0.440	2.831
1.80	0.452	2.882	0.454	2.967
1.97	0.518	2.940	0.519	3.015
2.20	0.504	2.983	0.505	3.073
2.40	0.475	2.999	0.477	3.088
2.60	0.479	3.000	0.480	3.053
2.80	0.482	2.999	0.483	3.091
3.00	0.485	2.999	0.486	3.082

Before presenting results for specific cases, it is helpful to recognize certain peculiar effects brought about by the presence of the inplane load. It is clear that since σ_d and σ_s are proportional to p_o while σ_y is independent of p_o, the DAF is not linearly proportional to p_o. In fact, as p_o increases the DAF decreases although the maximum stress increases. Further, the DAF is different from zero at $R = \bar{\bar{\tau}} = 0$ for which the dynamic effect would ordinarily be zero if there were no inplane loads.

i) No Time-lag

The envelopes of the DAF as a function of R are given in Fig. 2 for $Q_o/N_c = 1/4$ and 0 to illustrate the effect of the dynamic inplane load. The overpressure, p_o, is taken to be 1 psf and the duration of the inplane dynamic load is the same as the lateral N-shaped pulse ($\alpha = 1$). It is observed that the DAF is always higher when there is a dynamic inplane load.

In Fig. 3 the critical time, $\bar{t}_c$, for the maximum DAF corresponding to Fig. 2 is plotted as a function of R. It is seen that the presence of the dynamic inplane load tends to shift the time at which the maximum stress occurs from the free phase to the forced phase of the motion. When R is slightly above 1, the critical time, at which the maximum stress occurs, is always found to be in the compression phase of the N-shaped pulse. The practical implication is that except for a very flexible plate, the maximum stress always occurs at the beginning of the N-shaped disturbance due to the presence of the inplane disturbance.

The effect of a static inplane compressive load or prestress ($\tilde{N}_y/N_c = 1/4$) may be seen in Fig. 4 where the envelopes of DAF versus R are plotted. The maximum DAF is 5.7 for $Q_o/N_c = 1/4$ and 4.7 for $Q_o/N_c = 0$. Comparing Fig. 4 with Fig. 2, the increase in the maximum DAF due to the presence of the prestress is about 2.0 for R above 1.4. As in the previous case when the prestress is absent, the

DAF is always higher when there is a dynamic inplane load.

In Fig. 5, the critical time, $\bar{t}_c$, for the maximum DAF corresponding to Fig. 4 is plotted as a function of R. A similar trend is found as in Fig. 3, i.e., the critical time tends to be shifted to the forced phase.

In Fig. 6, the effects of increasing the duration of the dynamic inplane load is seen. It is observed that, in general, the longer duration ($\alpha = 2$) gives smaller DAF's; hence is less critical.

ii) With Time-lag

That the simultaneous application of lateral and inplane disturbances without a time-lag may not be the most likely case is obvious. Furthermore, it may not be the most critical case. Hence a time-lag is introduced into the linear problem to study the possible effects. It is decided to choose a relatively large value of R (R = 3) because it was discovered from the previous results that the DAF usually is stabilized at such a value of R. The results are presented in Table 3. It is clear that with a proper time-lag (positive or negative) the absolute maximum DAF is always larger in every case than the corresponding value for no time-lag. Corresponding to $Q_o/N_c = 1/4$, the maximum DAF could be larger than 6 when $\tilde{N}_y/N_c = 1/4$ and larger than 4 when $\tilde{N}_y/N_c = 0$. These DAF's are significantly larger than the corresponding DAF's, 4.04 and 2.65, when the dynamic inplane load is absent.

Table 3a. Maximum DAF and $\bar{t}_{cr}$ Corresponding to Negative Time-lag.

$p_o = 1$ $Q_o/N_c = 1/4$ $a/h = 240$

Loading Condition		$\bar{t}_o/\bar{\tau} = 0$		$\bar{t}_o/\bar{\tau} = -0.10$		$\bar{t}_o/\bar{\tau} = -0.25$	
		DAF	$\bar{t}_{cr}$	DAF	$\bar{t}_{cr}$	DAF	$\bar{t}_{cr}$
$\alpha = 1$	$\tilde{N}_y/N_c = 0$	3.50	.180	3.97	.168	3.25	.170
	$\tilde{N}_y/N_c = 1/4$	5.66	.220	6.02	.198	5.13	.180
$\alpha = 2$	$\tilde{N}_y/N_c = 0$	2.91	.160	3.33	.162	3.85	.165
	$\tilde{N}_y/N_c = 1/4$	4.92	.180	5.41	.180	6.00	.200

Table 3b. Maximum DAF and $\bar{t}_{cr}$ Corresponding to Positive Time-lag.

$p_o = 1$ $Q_o/N_c = 1/4$ $a/h = 240$

Loading Condition		$\bar{t}_o/\bar{\tau} = 0$		$\bar{t}_o/\bar{\tau} = 0.10$		$\bar{t}_o/\bar{\tau} = 0.25$	
		DAF	$\bar{t}_{cr}$	DAF	$\bar{t}_{cr}$	DAF	$\bar{t}_{cr}$
$\alpha = 1$	$\tilde{N}_y/N_c = 0$	3.50	.180	2.72	.170	2.67	.500
	$\tilde{N}_y/N_c = 1/4$	5.66	.220	4.64	.170	4.00	.175
$\alpha = 2$	$\tilde{N}_y/N_c = 0$	2.91	.160	3.10	.748	3.14	.684
	$\tilde{N}_y/N_c = 1/4$	4.92	.180	5.36	.874	5.92	.850

c) Response of Plate Based on Nonlinear Theory

The nonlinear model is constructed to include the mid-surface stretching of the plate. At the boundary of the plate, it is no longer sufficient to prescribe conditions governing the lateral displacement only. The inplane displacements (or tractions) must also be prescribed. In the previous chapter, two different boundary conditions are specified: movable vertical sides and immovable vertical sides. In both cases, the sides are to remain straight. Along the edge where the dynamic inplane load is transmitted, two sets of conditions are specified. One has the mass of the plate lumped along a rigid bar at the top of the plate ($k = 1$) and the other a rigid bar with no mass ($k = 0$). To simplify the problem for the nonlinear case, the lateral and inplane pulses are to have the same duration ($\alpha = 1$) and there is no time-lag.

In evaluating the time functions, the first three symmetric modes are computed and the contribution of higher modes are neglected. The membrane stress in the plate corresponding to the boundaries with movable sides becomes:

$$\sigma_y = \frac{E\pi^2}{8(a/h)^2}\Big\{ A^2(1-\cos 2\pi\bar{x}) + 2AC(\cos 2\pi\bar{x} - \cos 4\pi\bar{x}) \\ - 2AB\cos 2\pi\bar{x}\left(\cos 2\pi\bar{y} - \frac{1}{25}\cos 4\pi\bar{y}\right) \\ - 2AC\left(\cos 2\pi\bar{x} - \frac{1}{25}\cos 4\pi\bar{x}\right)\cos 2\pi\bar{y} \\ - \frac{8a}{\pi^2 h}\,\varphi_y(\bar{t})\Big\} \qquad (4.4)$$

and the membrane stress corresponding to the immovable vertical sides becomes:

$$\sigma_y = \frac{E\pi^2}{8(a/h)^2}\Big\{\frac{A^2}{1-\nu^2} - A^2\cos 2\pi\bar{x} + 2AC(\cos 2\pi\bar{x} - \cos 4\pi\bar{x})$$

$$- 2AB\cos 2\pi\bar{x}\,(\cos 2\pi\bar{y} - \frac{1}{25}\cos 4\pi\bar{y})$$

$$- 2AC\,(\cos 2\pi\bar{x} - \frac{4}{25}\cos 4\pi\bar{x})\cos 2\pi\bar{y}$$

$$- \frac{8a}{\pi^2 h(1-\nu^2)}\,\varphi_y(\bar{t})\Big\} \tag{4.5}$$

The dynamic bending stress is evaluated by the same equation, (4. 2), as in the linear model.

The problem with the movable vertical sides was solved numerically for k = 0 (no mass on top) and k = 1 (with mass on top) when the prestress was absent. The maximum deflections and stresses obtained were found to be almost identical.

If (3. 21), for the movable vertical sides, is linearized, the solution for quiescent initial conditions is:

$$\varphi_y = \frac{4\pi^2}{12(a/h)(1-\nu^2)}\,\frac{\tilde{N}_y}{N_c}\left(1 - \cos\sqrt{\frac{12(1-\nu^2)}{k}}\,\frac{a\bar{t}}{\pi h}\right)$$

$$+ \frac{4a/(kh)}{\dfrac{12a^2(1-\nu^2)}{\pi^2h^2k} - \left(\dfrac{2\pi}{\alpha\bar{\tau}}\right)^2}\,\frac{Q_o}{N_c}\left[\sin\frac{2\pi\bar{t}}{\alpha\bar{\tau}} - \frac{2\pi/(\alpha\bar{\tau})}{\sqrt{\dfrac{12(1-\nu^2)}{k}}\,\dfrac{a}{\pi h}}\,\sin\sqrt{\frac{12(1-\nu^2)}{k}}\,\frac{a\bar{t}}{\pi h}\right]. \tag{4.6}$$

With $a/h = 240$, $\nu = 0.231$, $k = 1$, $\alpha = 1$, and $\bar{\tau}$ greater than 0.1, (4.6) is approximately equal to

$$\varphi_Y = \frac{4\pi^2}{12\, a/h\,(1-\nu^2)} \left[\frac{\tilde{N}_Y}{N_c} (1 - \cos 80\pi \bar{t}) + \frac{Q_o}{N_c} \left(\sin \frac{2\pi \bar{t}}{R} - \frac{1}{40R} \sin 80\pi\bar{t} \right) \right] . \quad (4.6a)$$

If the inertia of the loading bar is neglected, the solution to the linearized form of (3.21) is

$$\varphi_Y = \frac{4\pi^2}{12(a/h)(1-\nu^2)} \left[\frac{\tilde{N}_Y}{N_c} + \frac{Q_o}{N_c} \sin \frac{2\pi \bar{t}}{R} \right] \quad (4.7)$$

If $\tilde{N}_y/N_c = 0$, the two solutions are approximately equal provided $\frac{1}{40\,R}$ is much less than unity. This is true except for very small R. Therefore it seems that the longitudinal inertia can be neglected if R is not too small and there is no prestress. In the subsequent discussion both the longitudinal inertia and the prestress will not be considered.

The maximum DAF for the movable vertical sides as a function of R is given in Fig. 7 for $p_o = 1$ and in Fig. 8 for $p_o = 2$. Comparing Fig. 7 with Fig. 8, the effect of the inplane dynamic load on the maximum DAF is seen to be less for $p_o = 2$ when R is greater than 1.2.

The maximum DAF as a function of R is plotted for the immovable and movable boundaries in Fig. 9 for $Q_o/N_c = 0$ and $p_o = 2$. Fig. 9 shows that the maximum DAF is always larger for the movable boundaries than for the immovable boundaries. This is not surprising since the lateral deflection of a plate exposed to a lateral load only should be larger when the boundaries are allowed to move. However in Fig. 10, where all the conditions on the plate are the same as in Fig. 9 except $Q_o/N_c = 1/4$, it is seen that the DAF for the movable boundaries may be, depending on R, larger or smaller than the DAF for the immovable boundaries. It is noted that for the entire range of R, whether there is an inplane dynamic pulse or not, there is very little difference between the maximum DAF's for the movable and immovable boundary conditions.

d) Comparison of Linear and Nonlinear Theories

The dynamic bending stress, σ_d, is no longer proportional to p_o in the nonlinear model as it was in the linear model. Furthermore, there is a membrane stress due to the mid-surface stretching. As a result, the stress distributions through the thickness of the plate are different for the two models. However, if one is interested in the maximum stress which always occurs on the surface of the plate, some meaningful comparison can be made of the two models. In order to make the comparison, the contribution of the first three modes is used for both models. The decrease in the number of modes used does not significantly change the results of the linear model as was demonstrated in Table 2.

If the equations (3.18-3.20, 3.22) which are for the movable boundaries with the inertia of the rigid bar neglected are linearized, the resulting equations (2.9) are those obtained by the linear theory. Therefore, for the purpose of comparison, the curves presented for the nonlinear model are for the movable boundaries.

The envelopes of $\bar{w}$ as a function of p_o are given in Fig. 12 for $R = 1$. Q_o/N_c is taken to be 0 and 1/4. It is seen that at a value of $\bar{w}$ approximately equal to 0.5, the linear and nonlinear deflections differ only by about 10%. Of course, the difference becomes magnified as $\bar{w}$ increases. It is also noted that the effect of the inplane pulse on the deflections is more or less constant for the nonlinear model at large $\bar{w}$.

If the curves for the maximum DAF in Fig. 7 are now compared to those of Fig. 2, obtained by the linear theory, one sees that they are almost identical. This is not surprising since the deflection in this case is always less than 0.3. This indicates that the results of the linear theory are still accurate.

In Fig. 13, the envelopes of the deflection versus R with $Q_o/N_c = 1/4$ and $p_o = 2$ are shown. It is seen that the deflections (the maximum of which is about 0.6) for the linear model are about 10% larger than the deflections for the nonlinear model. Therefore, one would expect that the stresses predicted by the linear model may be more than 10% higher than what is predicted by the nonlinear model. This is verified in Fig. 14 where the envelopes of the DAF are plotted. If a 10% error is tolerated, it seems that the validity of the linear theory should be confined to a value of $\bar{w}$ less than one-half.

It is noted from Fig. 14 that for R less than 1.2, the DAF of the nonlinear model is larger than the DAF of the linear model. This is due to the fact that when R is less than 1.2, the critical time occurs after the dynamic inplane pulse is off the plate. Apparently the membrane stress in the nonlinear model more than offsets the difference in the bending stress which, as the deflection, is larger in the linear model.

In Fig. 15 the envelopes of the deflection versus R are shown for $p_o = 10$ for the same plate. Unlike the results shown in Fig. 13, the deflection of the linear model is much larger than the deflection of the nonlinear model. Obviously, one would not expect the stresses predicted by the linear theory to be acceptable. However, even the Von Kármán's nonlinear theory predicts the maximum deflection on the order of one and a half to twice the plate thickness. The question naturally arises as to whether the results of the nonlinear model are valid. A higher order nonlinear theory may be necessary.

Chapter 5. Summary and Conclusions

The transient response of a simply supported rectangular plate subjected to a dynamic inplane load in the form of a sine pulse and to a lateral N-shaped pressure pulse is examined. The imposition of the lateral and inplane disturbances may be simultaneous or separated by a brief time-delay. In addition, there may be a static inplane compressive load. The support of the plate is such that no tensile inplane load is transmitted to the plate. The problem simulates a window pane exposed to the effects of a far-field sonic boom disturbance with the inplane load transmitted from the roof structure.

The problem is studied first by a small deflection or linear theory. The governing partial differential equation of motion is reduced to a set of ordinary differential equations by assuming mode shapes that satisfy the boundary conditions. Due to the presence of the inplane dynamic load in the form of a sine pulse, the equations of motion are of the Mathieu type. Following McLachlan, the solution is obtained in terms of Mathieu functions of fractional order. However, the existing method does not always insure an accurate determination of the coefficients in the series solution as can be seen in Table 1. An improved procedure is presented by which for all the cases encountered, the coefficients in the series solution are always correctly determined.

The convergence of the linear solutions is demonstrated by using a three mode and a nine mode expansion. It is seen in Table 2 that reliable results can be obtained by considering just the first three modes. As expected, the inplane dynamic load induces substantially higher stress in the plate (see Fig. 2 and Fig. 4). In addition, Table 3 shows that the time-delay can cause a substantial increase in the dynamic amplification factor or dynamic stress.

Since the lateral deflection of the plate can reach such a magnitude as to render the results of the linear theory in doubt, a nonlinear theory, which takes into account the stretching of the mid-surface of the plate, is used. The equations of motion and the associated boundary conditions are derived in the Appendix using Hamilton's principle.

In the nonlinear theory, in addition to the usual simply supported boundary conditions, the problem is posed for two different inplane boundary conditions: movable vertical sides and immovable vertical sides. For both sets of inplane boundary conditions, the longitudinal inertia of the plate is either neglected or considered by assuming that all the longitudinal mass is concentrated at the top of the plate. A three mode expansion for the lateral deflection is proposed and the inplane displacements are determined in terms of the lateral deflection. The equation of motion is reduced to a system of ordinary nonlinear coupled differential equations by the Galerkin method. These equations are then solved numerically using Hamming's modified predictor-corrector integration method. It is found that if the static inplane load is absent, the solutions are almost identical whether the longitudinal mass is neglected or when it is assumed to be concentrated at the top. The effect of the two different inplane boundary conditions namely, movable and immovable vertical sides, is shown in Fig. 9 for $Q_o/N_c = 0$ and in Fig. 10 for $Q_o/N_c = 1/4$. It is seen that the maximum stresses at the center of the plate are approximately the same for either boundary condition.

When the equations of motion corresponding to the case of movable vertical sides and no longitudinal inertia are linearized, the resulting equations are exactly those of the linear theory. Therefore for the purpose of comparison, the results for the movable vertical sides are used. It is found that for $p_o = 1$ psf, the results of the linear and nonlinear theories are almost identical. This is not surprising since the lateral deflection in this case is always less than 0.3 of the thickness of the plate. For $p_o = 2$ psf, however, it is found that the deflections obtained by the linear theory can be more than 10% larger than those obtained by the nonlinear theory. Therefore the stresses predicted by the linear theory can be more than 10% off than that predicted by the nonlinear theory. One may conclude, therefore, that if a 10% error is tolerated, the linear theory gives acceptable results if the lateral deflection is confined to be less than one-half the thickness of the plate.

Appendix Derivation of Nonlinear Equations of Motion and Boundary Conditions Using Hamilton's Principle

In addition to the usual assumptions for a thin elastic plate, it is assumed that

a) the magnitude of the lateral deflection, w, is of the same order of magnitude as the thickness of the plate;

b) the tangential displacements u and v are infinitesimal so that the only significant nonlinear terms in the strain-displacement equations are $w_{,x}$ and $w_{,y}$.

Then the middle surface strains are given by:

$$\begin{aligned}
\varepsilon_{xxo} &= u_{,x} + \tfrac{1}{2}(w_{,x})^2 \\
\varepsilon_{yyo} &= v_{,y} + \tfrac{1}{2}(w_{,y})^2 \\
\varepsilon_{xyo} &= u_{,y} + v_{,x} + w_{,x}\, w_{,y} \\
\varepsilon_{xzo} &= \varepsilon_{yzo} = \varepsilon_{zzo} = 0
\end{aligned} \tag{A.1}$$

and the strains at any point are given by:

$$\begin{aligned}
\varepsilon_{xx} &= \varepsilon_{xxo} - z\, w_{,xx} \\
\varepsilon_{yy} &= \varepsilon_{yyo} - z\, w_{,yy} \\
\varepsilon_{xy} &= \varepsilon_{xyo} - 2z\, w_{,xy} \\
\varepsilon_{xz} &= \varepsilon_{yz} = \varepsilon_{zz} = 0 \quad .
\end{aligned} \tag{A.2}$$

Furthermore, it will be assumed that the strains are small so that Hooke's Law applies:

$$\sigma_{xx} = \frac{E}{1-\nu^2}(\varepsilon_{xx} + \nu\,\varepsilon_{yy})$$
$$\sigma_{yy} = \frac{E}{1-\nu^2}(\varepsilon_{yy} + \nu\,\varepsilon_{xx}) \tag{A. 3}$$
$$\sigma_{xy} = \frac{E}{2(1+\nu)}\varepsilon_{xy}$$

Hamilton's principle states:

$$\delta\int_{t_1}^{t_2}(T - U + W)\,dt = 0, \tag{A. 4}$$

which means that the integral of the lagrangian function (L=U-T-W) over a time interval t_1 to t_2 is an extremum for the actual motion with respect to all admissable virtual displacements. These virtual displacements vanish at the initial and final configurations. It is noted that T is the kinetic energy of the body; U is the total strain energy of the body; and W is the work done by the external forces. For a linearly elastic material

$$U = \frac{1}{2}\int_V \sigma_{ij}\,\varepsilon_{ij}\,dV\,. \tag{A. 5}$$

Substituting (A. 1), (A. 2) and (A. 3) into (A. 5) and integrating through the thickness yields

$$U = \int_S \frac{1}{2}\Big[N_x u_{,x} + N_y v_{,y} + N_{xy}(u_{,y} + v_{,x})$$

$$+ \frac{1}{2}(N_x w_{,x}^2 + N_y w_{,y}^2 + 2 N_{xy} w_{,x} w_{,y})$$

$$+ D \{ (w_{,xx} + \nu w_{,yy}) w_{,xx} + (w_{,yy} + \nu w_{,xx}) w_{,yy}$$

$$+ 2(1-\nu) w_{,xy} \} \Big] dS \, , \qquad \text{(A. 6)}$$

where

$$N_x = \frac{Eh}{1-\nu^2} (\varepsilon_{xxo} + \nu \varepsilon_{yyo})$$

$$N_y = \frac{Eh}{1-\nu^2} (\varepsilon_{yyo} + \nu \varepsilon_{xxo})$$

$$N_{xy} = \frac{Eh}{2(1+\nu)} \varepsilon_{xyo}$$

$$D = \frac{Eh^3}{12(1-\nu^2)} \qquad \text{(A. 7)}$$

If the plate is loaded by a distributed lateral load, $q(x, y, t)$; normal and tangential inplane loads, N_n and N_t; bending and twisting moments, M_n and M_{nt}; and a transverse shearing force, Q_n; (as shown in Fig. 16) the external work done by these forces is:

$$W = \int_{\mathcal{S}} q\, w \, d\mathcal{S} - \int_c M_n w_{,n} \, dc - \int_c M_{nt,c} \, w \, dc + \int_c Q_n w \, dc + \int_c N_n (u \cos\theta + v \sin\theta) \, dc + \int_c N_t (v \cos\theta - u \sin\theta) \, dc . \qquad \text{(A. 8)}$$

The kinetic energy of the plate is given by:

$$T = \frac{\mu}{2} \int_{\mathcal{S}} (\dot{u}^2 + \dot{v}^2 + \dot{w}^2) \, d\mathcal{S} . \qquad \text{(A. 9)}$$

Substituting (A. 6), (A. 7), (A. 8) and (A. 9) into (A. 4) and integrating by parts yields:

$$\begin{aligned}
\int_{t_1}^{t_2} \Big\{ \int_{\mathcal{S}} & [(-\mu \ddot{w} - D\nabla^4 w + N_x w_{,xx} + 2N_{xy} w_{,xy} + N_y w_{,yy} \\
& + w_{,x}(N_{x,x} + N_{xy,y}) + w_{,y}(N_{xy,x} + N_{y,y}) + q)\,\delta w \\
& + (N_{x,x} + N_{xy,y} - \mu \ddot{u})\,\delta u + (N_{xy,x} + N_{y,y} - \mu \ddot{v})\,\delta v] \, d\mathcal{S} \\
+ \int_c \Big\{ & [-D(1-\nu)(w_{,xx}\cos^2\theta + 2w_{,xy}\sin\theta\cos\theta + w_{,yy}\sin^2\theta) \\
& - D\nu \Delta w - M_n] \frac{\partial}{\partial n}(\delta w) \\
& + [-D(1-\nu)\frac{\partial}{\partial c}\{(w_{,xx} - w_{,yy})\sin\theta\cos\theta + w_{,xy}(\sin^2\theta - \cos^2\theta)\} \\
& + D(\Delta w_{,x}\cos\theta + \Delta w_{,y}\sin\theta) \\
& - (N_{nn} w_{,n} + N_{cn} w_{,c}) + Q_n - M_{nt,c}]\,\delta w \qquad \text{(A. 10)} \\
& + (-N_{nn} + N_n)\,\delta n + (-N_{tn} + N_t)\,\delta t \Big\} dc \Big\} dt = 0.
\end{aligned}$$

Since all of the virtual displacements are arbitrary, from the fundamental theorem of calculas of variation each of the integrands in equation (A. 10) must vanish separately. This yields the following differential equations:

$$D\nabla^4 w = -\mu \ddot{w} + q + N_x w_{,xx} + 2N_{xy} w_{,xy} + N_y w_{,yy}$$
$$+ w_{,x}(N_{x,x} + N_{xy,y}) + w_{,y}(N_{xy,x} + N_{y,y})$$

$$N_{x,x} + N_{xy,y} - \mu \ddot{u} = 0 \qquad \text{(A. 11)}$$

$$N_{xy,x} + N_{y,y} - \mu \ddot{v} = 0$$

and the boundary conditions on the boundary c:

$$D[(1-\nu)(w_{,xx}\cos^2\theta + 2w_{,xy}\sin\theta\cos\theta + w_{,yy}\sin^2\theta) + \nu\Delta w]$$
$$+ M_n = 0 \qquad \text{or} \qquad \delta(w_{,n}) = 0$$

$$D[(1-\nu)\frac{\partial}{\partial c}\left((w_{,xx} - w_{,yy})\sin\theta\cos\theta + w_{,xy}(\sin^2\theta - \cos^2\theta)\right)$$
$$- \frac{\partial}{\partial x}(\Delta w)\cos\theta - \frac{\partial}{\partial y}(\Delta w)\sin\theta]$$
$$+ (N_x\cos^2\theta + 2N_{xy}\sin\theta\cos\theta + N_y\sin^2\theta)w_{,n}$$
$$+ (-N_x\sin\theta\cos\theta + N_{xy}(\cos^2\theta - \sin^2\theta) + N_y\sin\theta\cos\theta)w_{,c}$$
$$- Q_n + \frac{\partial M_{nt}}{\partial c} = 0 \qquad \text{or} \qquad \delta w = 0$$

$$N_x\cos^2\theta + 2N_{xy}\sin\theta\cos\theta + N_y\sin^2\theta = N_n \qquad \text{or} \qquad \delta n = 0$$
$$(-N_x\sin\theta\cos\theta + N_{xy}(\cos^2\theta - \sin^2\theta) + N_y\sin\theta\cos\theta) = N_t \qquad \text{or} \; \delta t = 0.$$

These results were first obtained by Herrman [18].

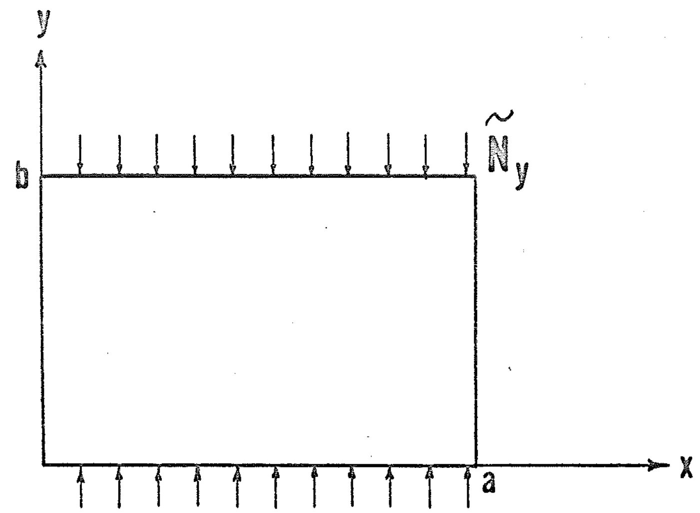

Rectangular Plate with Static Inplane Load

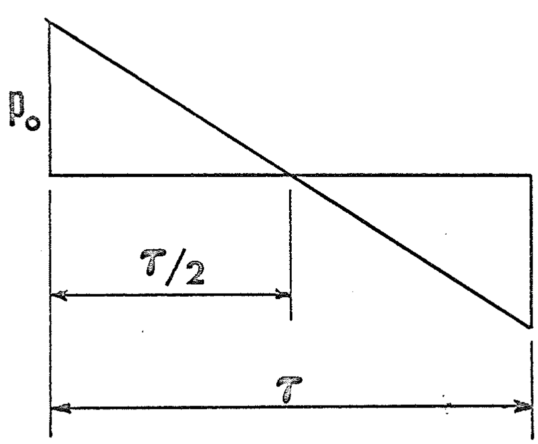

Lateral N-Shaped Disturbance

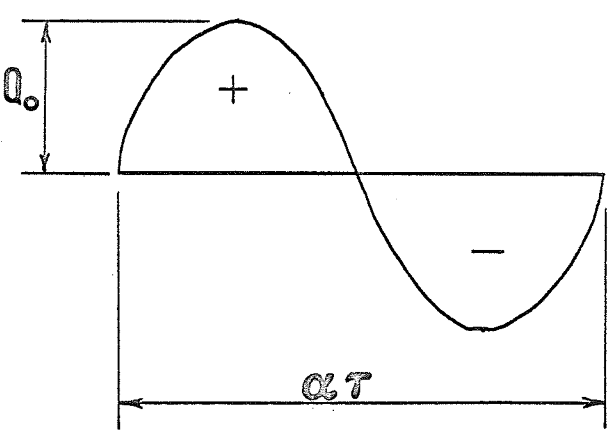

Inplane Disturbance

Figure 1

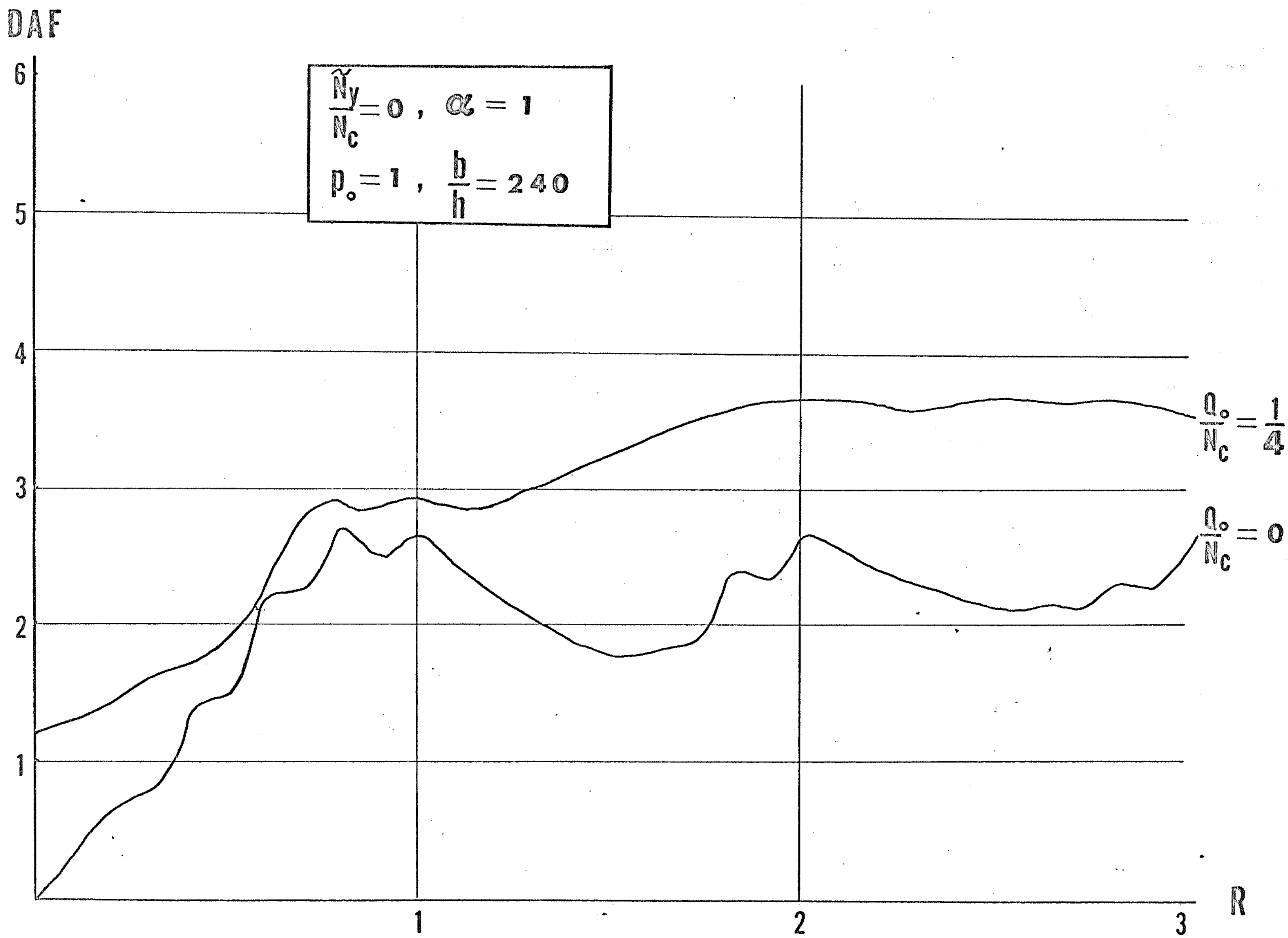

Fig. 2

DAF vs. Period Ratio of a Square Plate

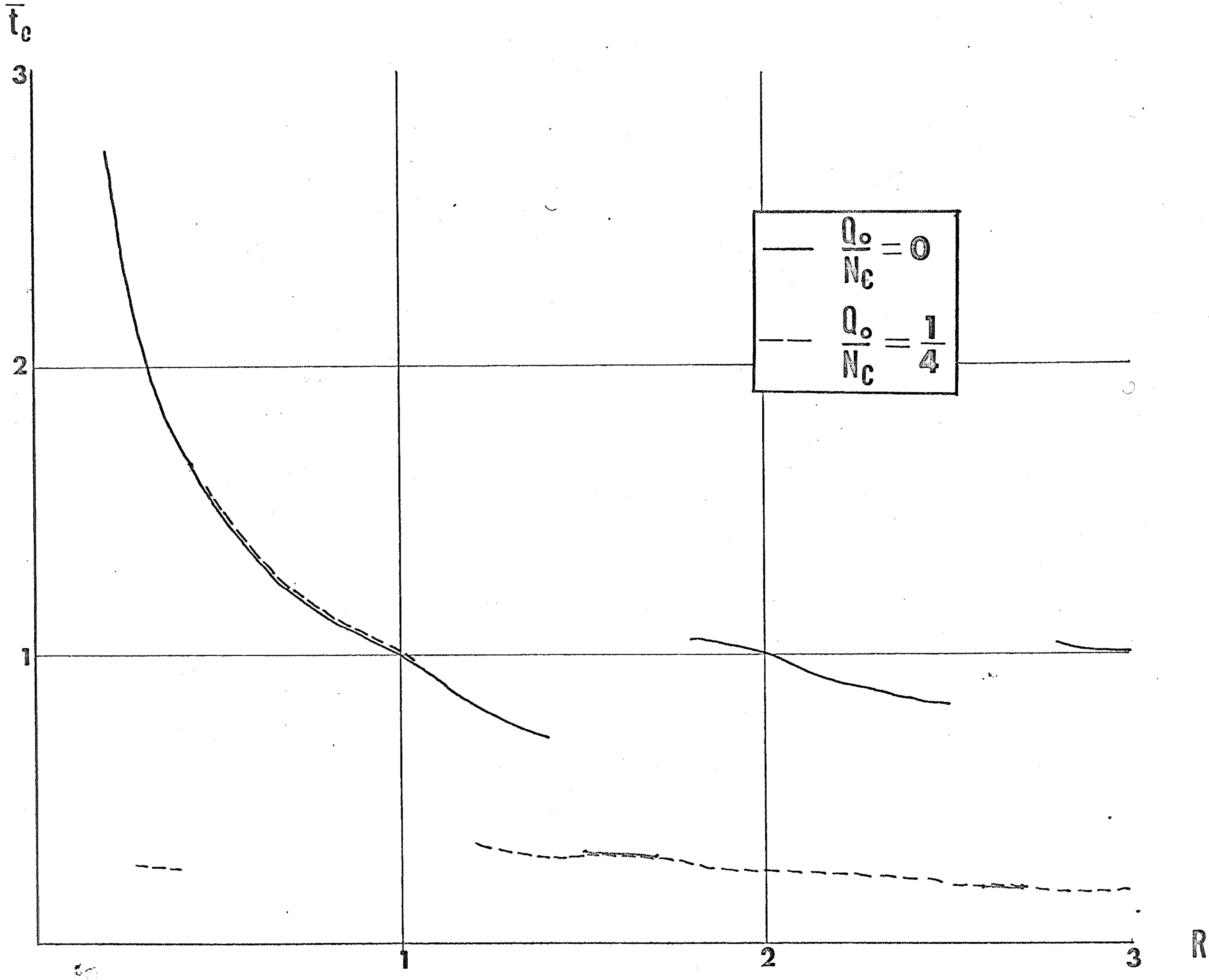

Fig. 3 Critical Time Corresponding to Fig. 2

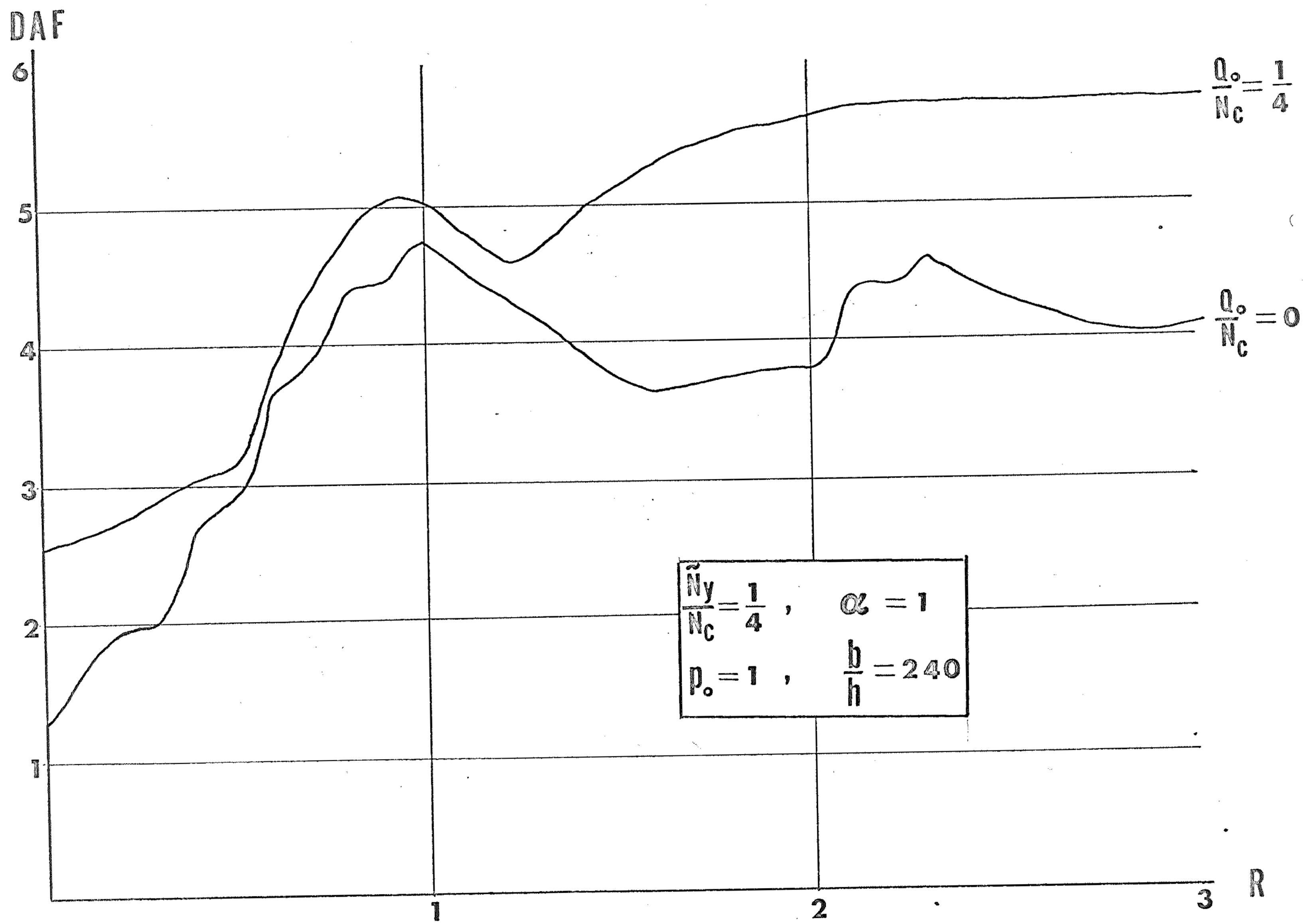

Fig. 4 DAF vs. Period Ratio of a Square Plate

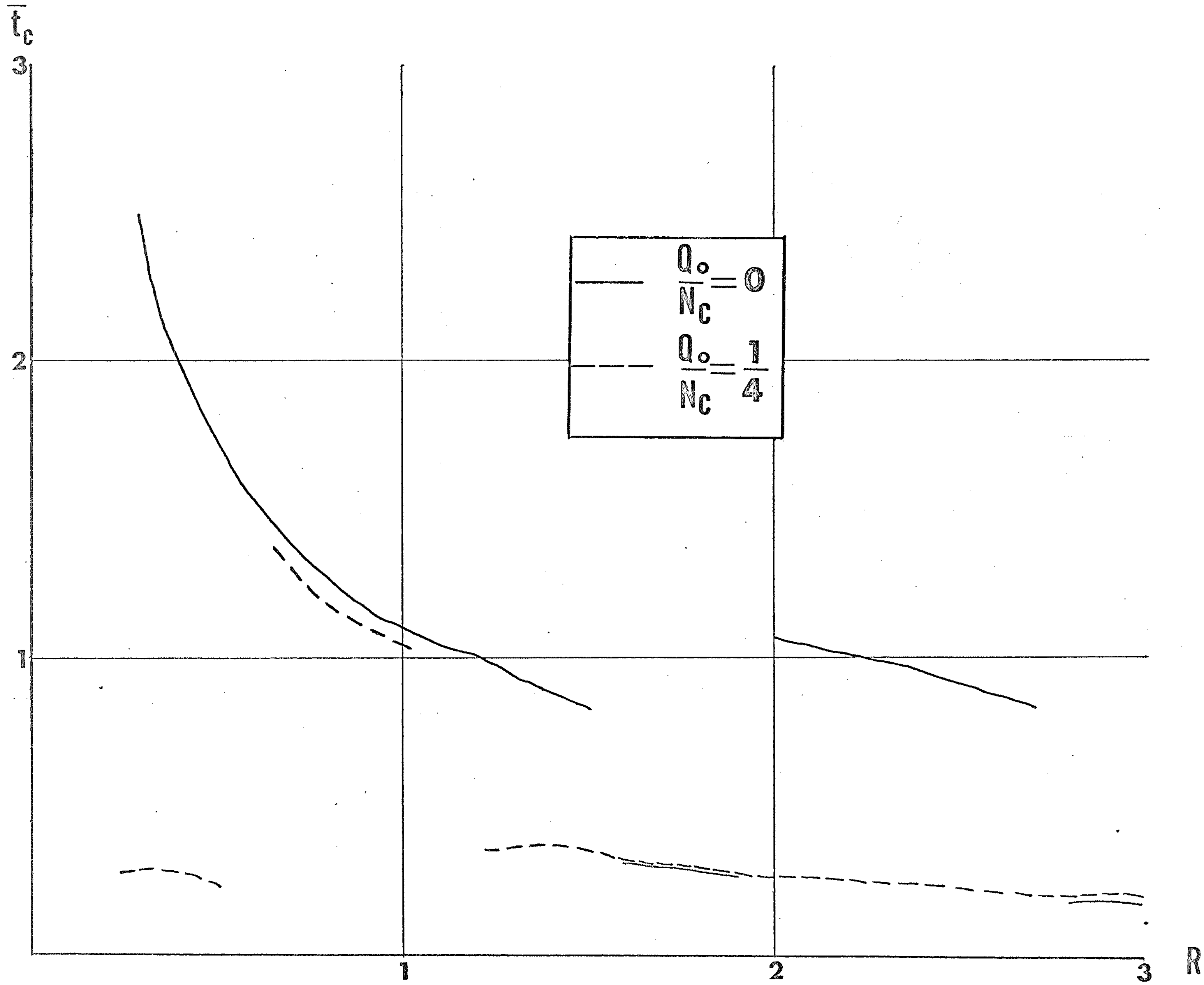

Fig. 5 Critical Time Corresponding to Fig. 4

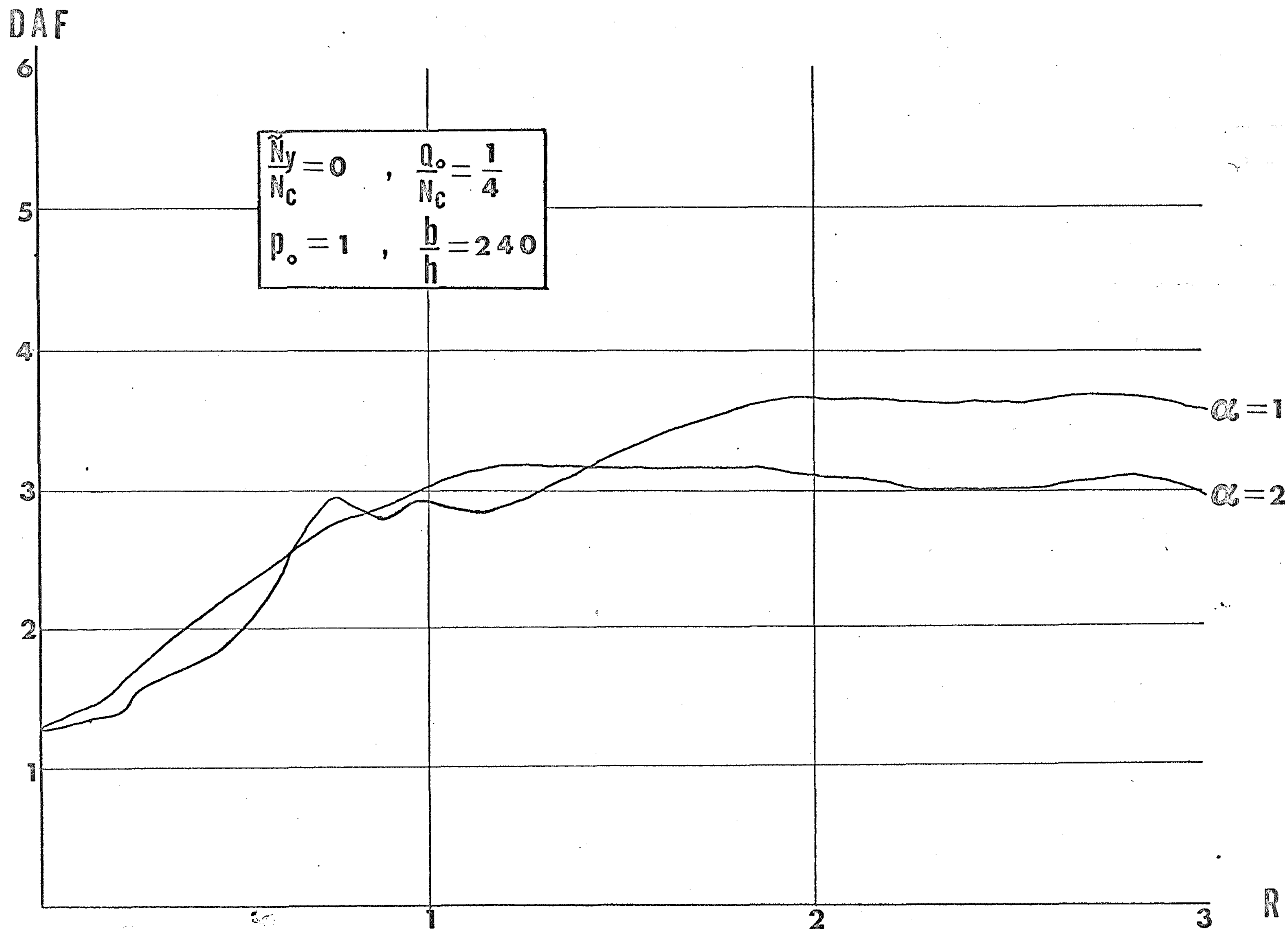

Fig. 6 Effect of Duration of Inplane Dynamic Load — No Static Inplane Load

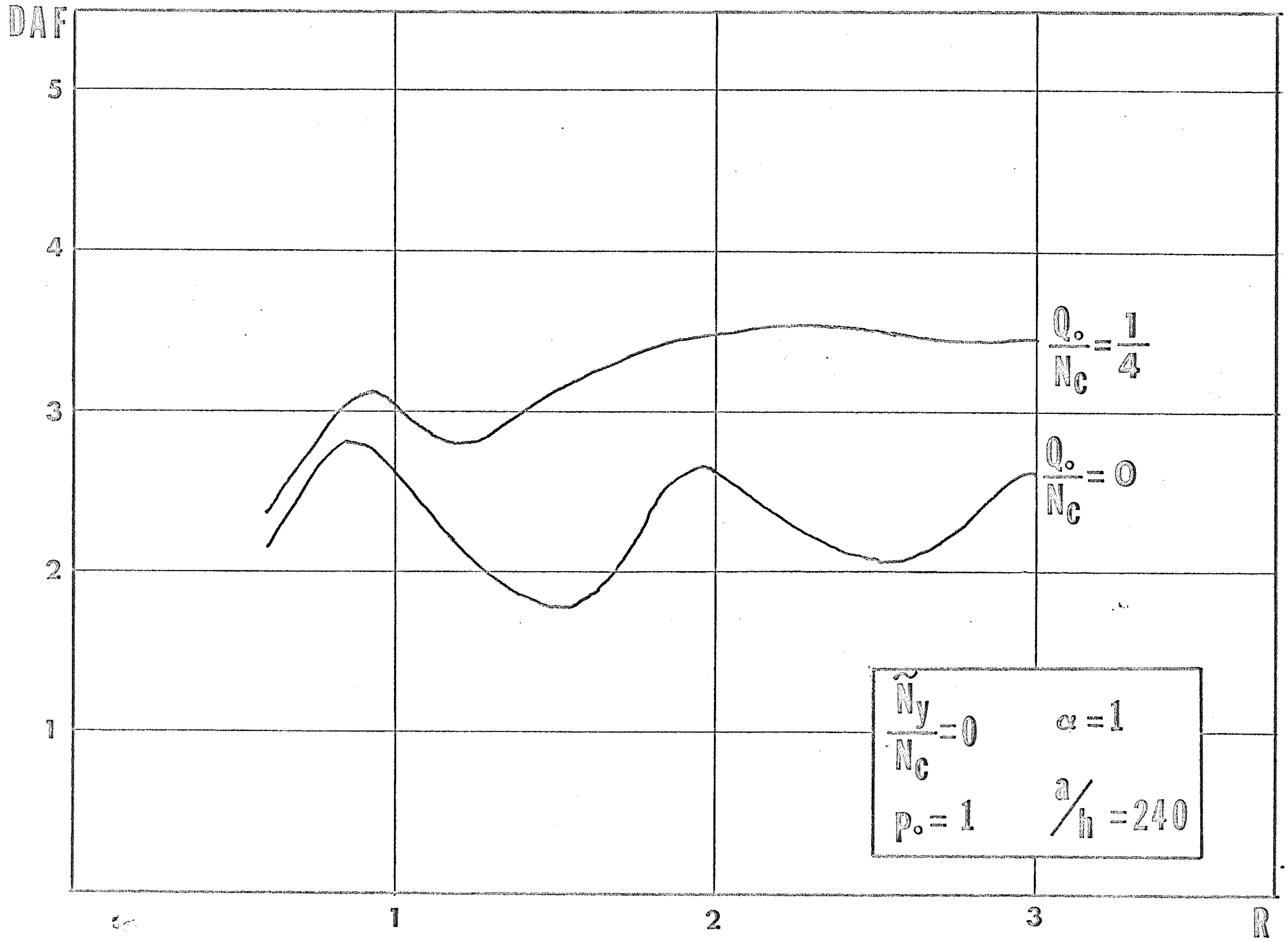

Fig. 7 DAF vs Period Ratio of a Square Plate

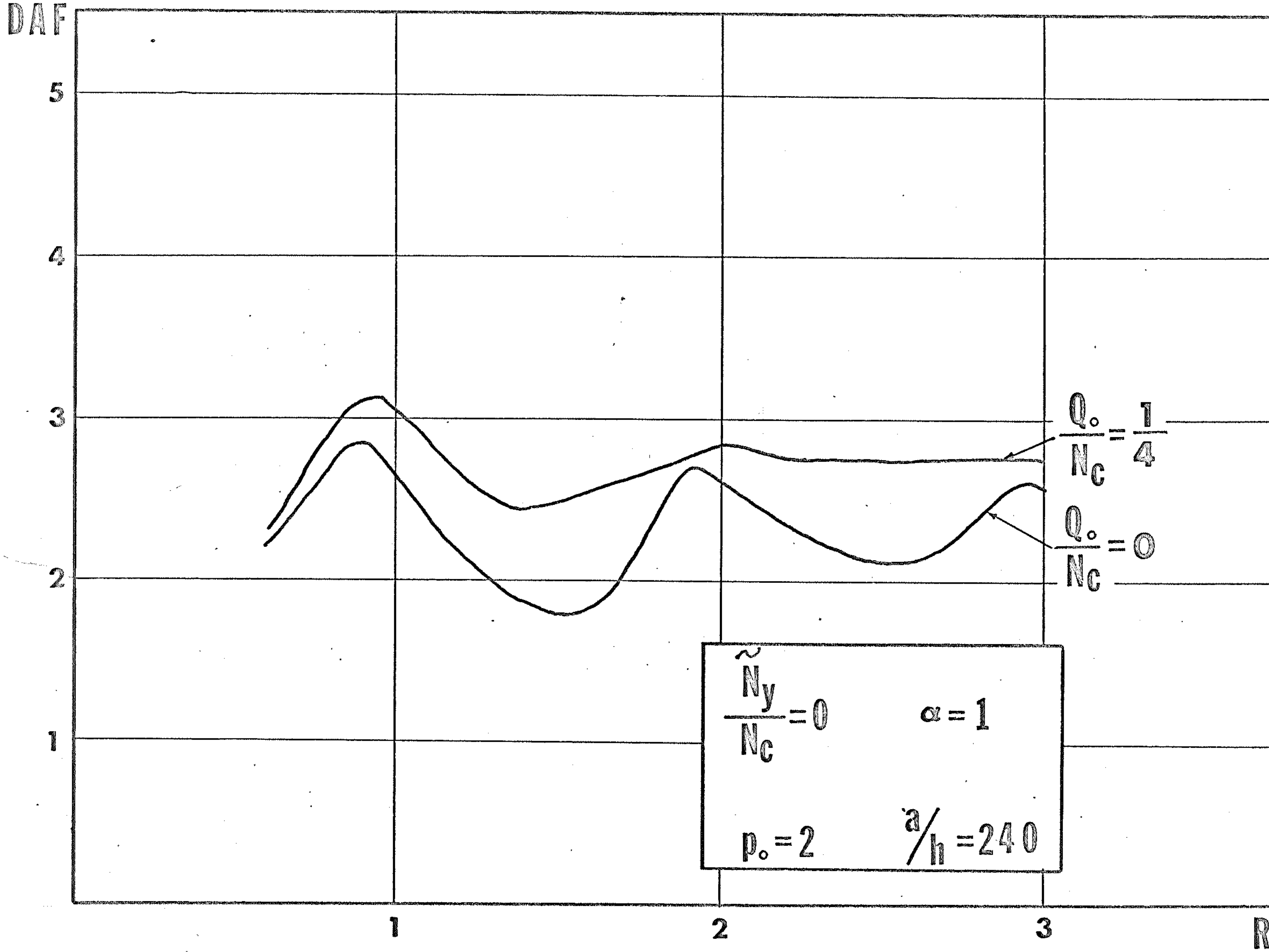

Fig. 8 DAF vs Period Ratio of a Square Plate

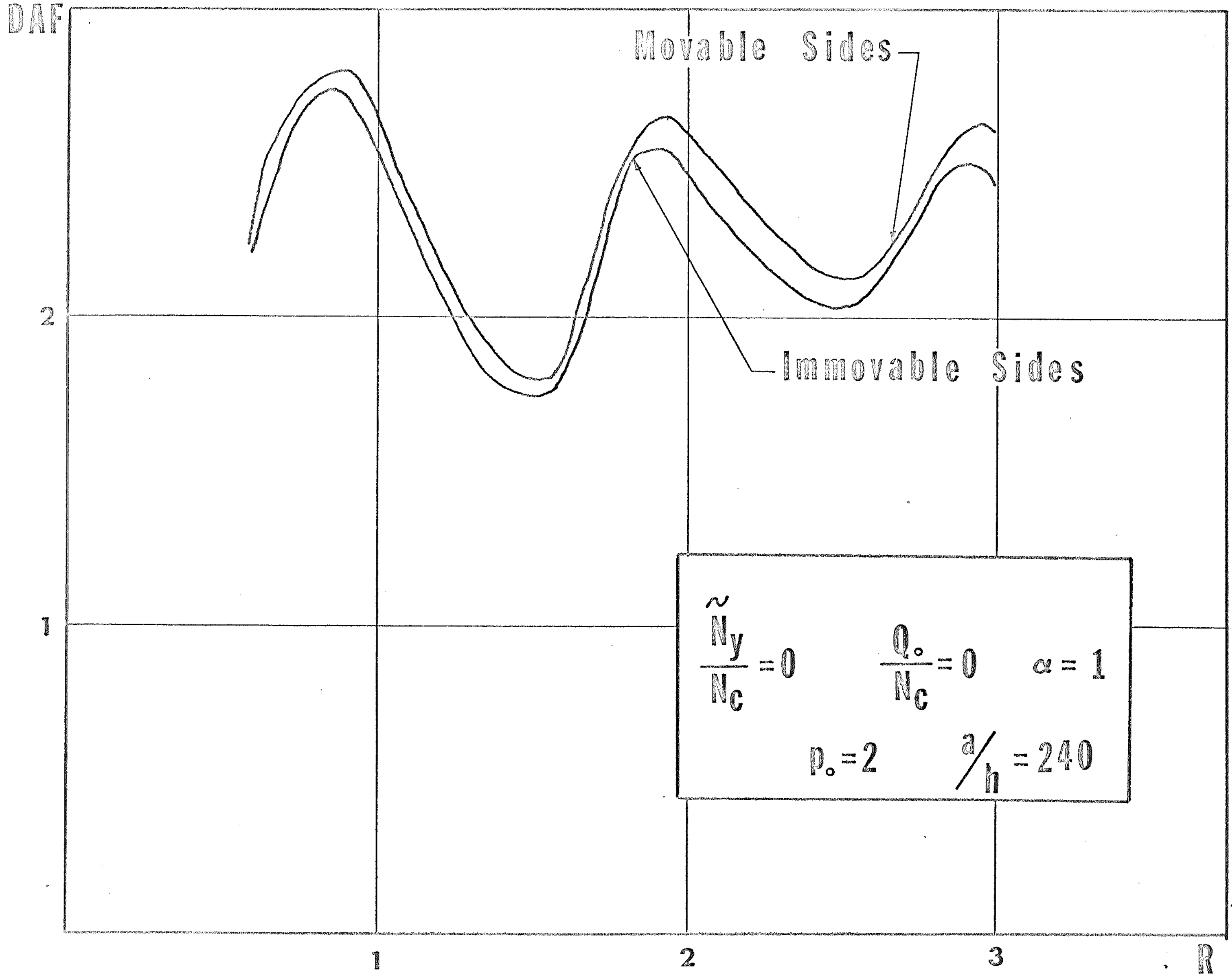

Fig.9 Effect of Boundary Conditions

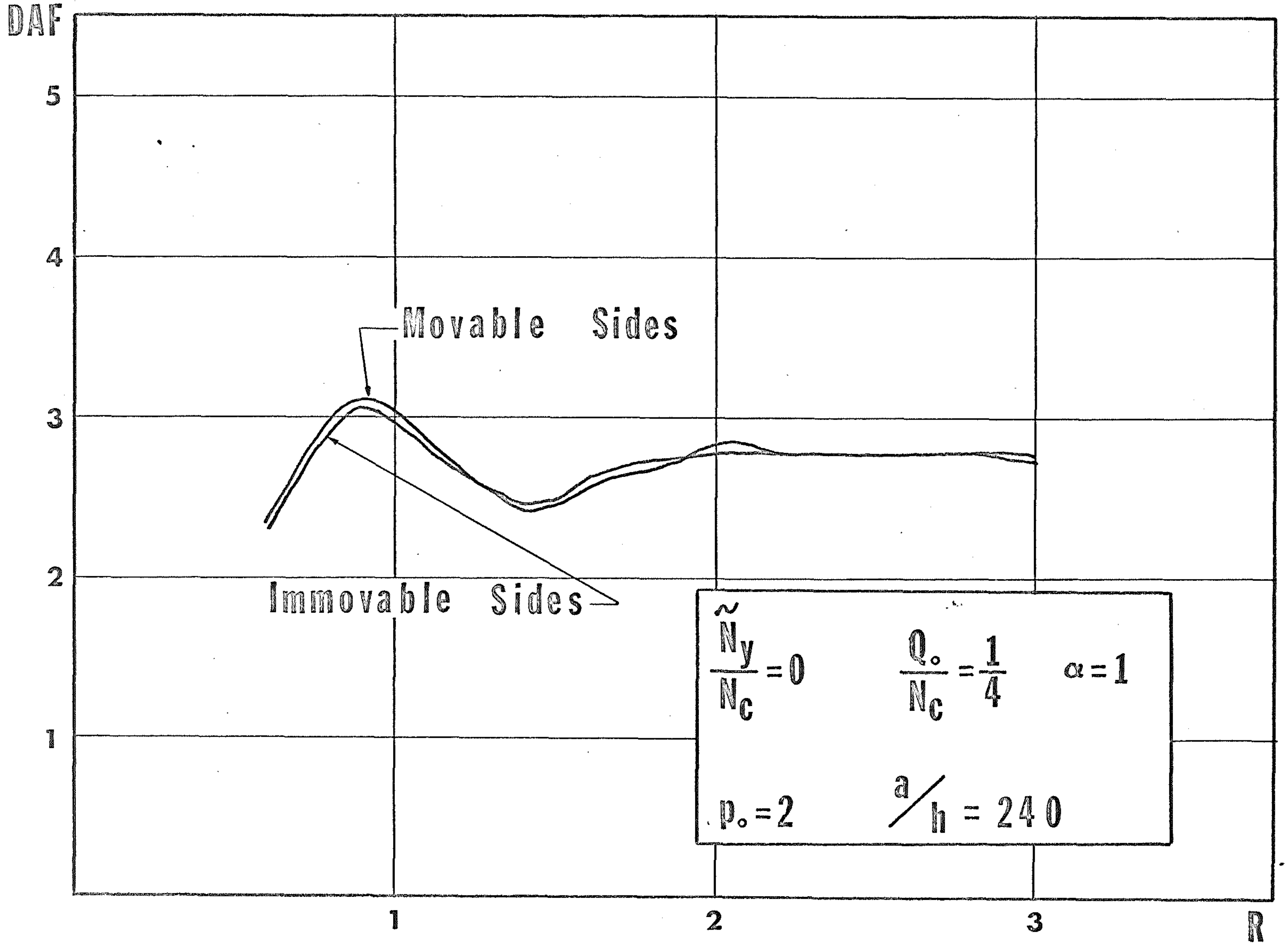

Fig. 10 Effect on Boundary Conditions

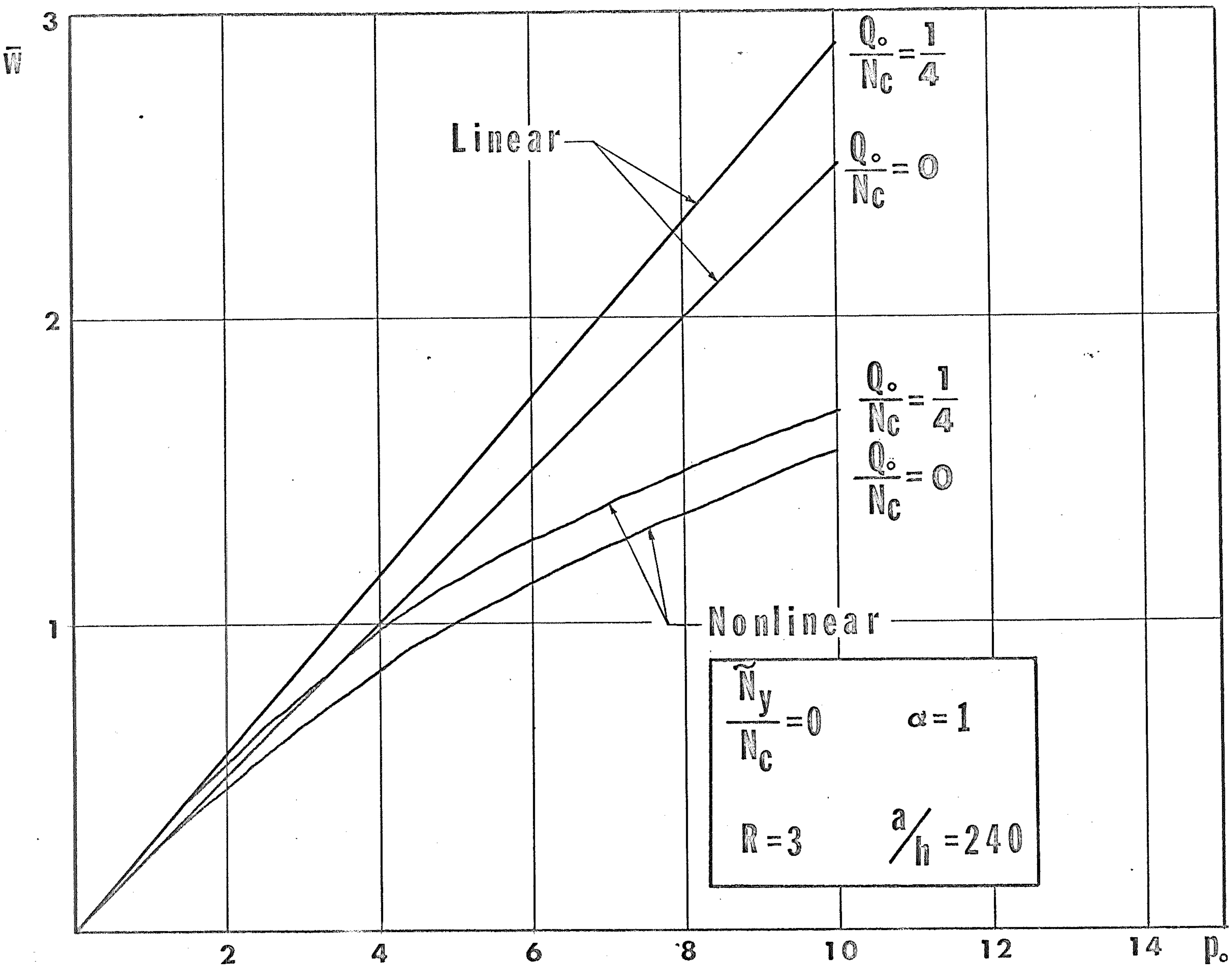

Fig. 11 $\bar{w}$ vs p_o for a Square Plate

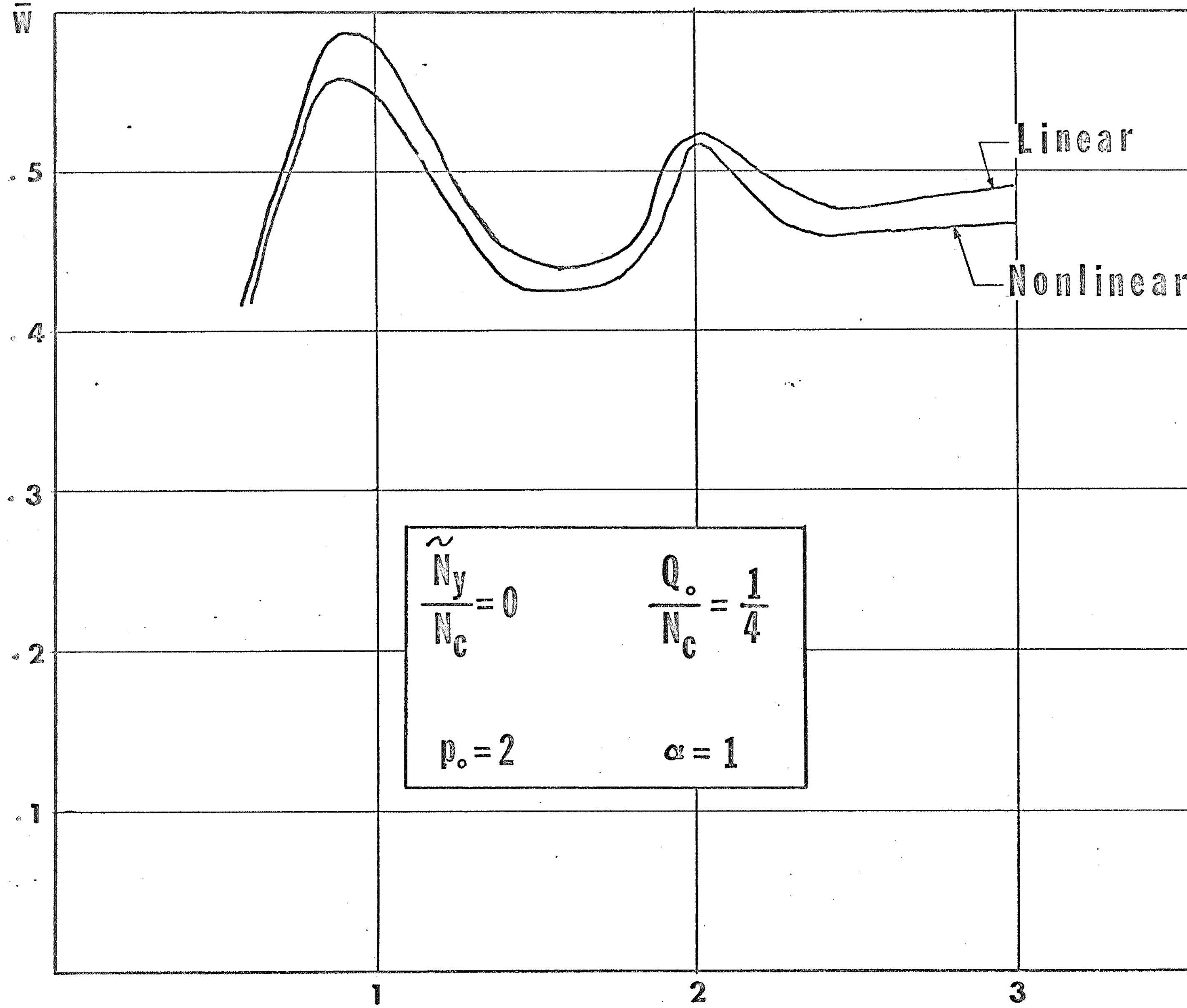

Fig.12 $\bar{w}$ vs Period Ratio for a Square Plate

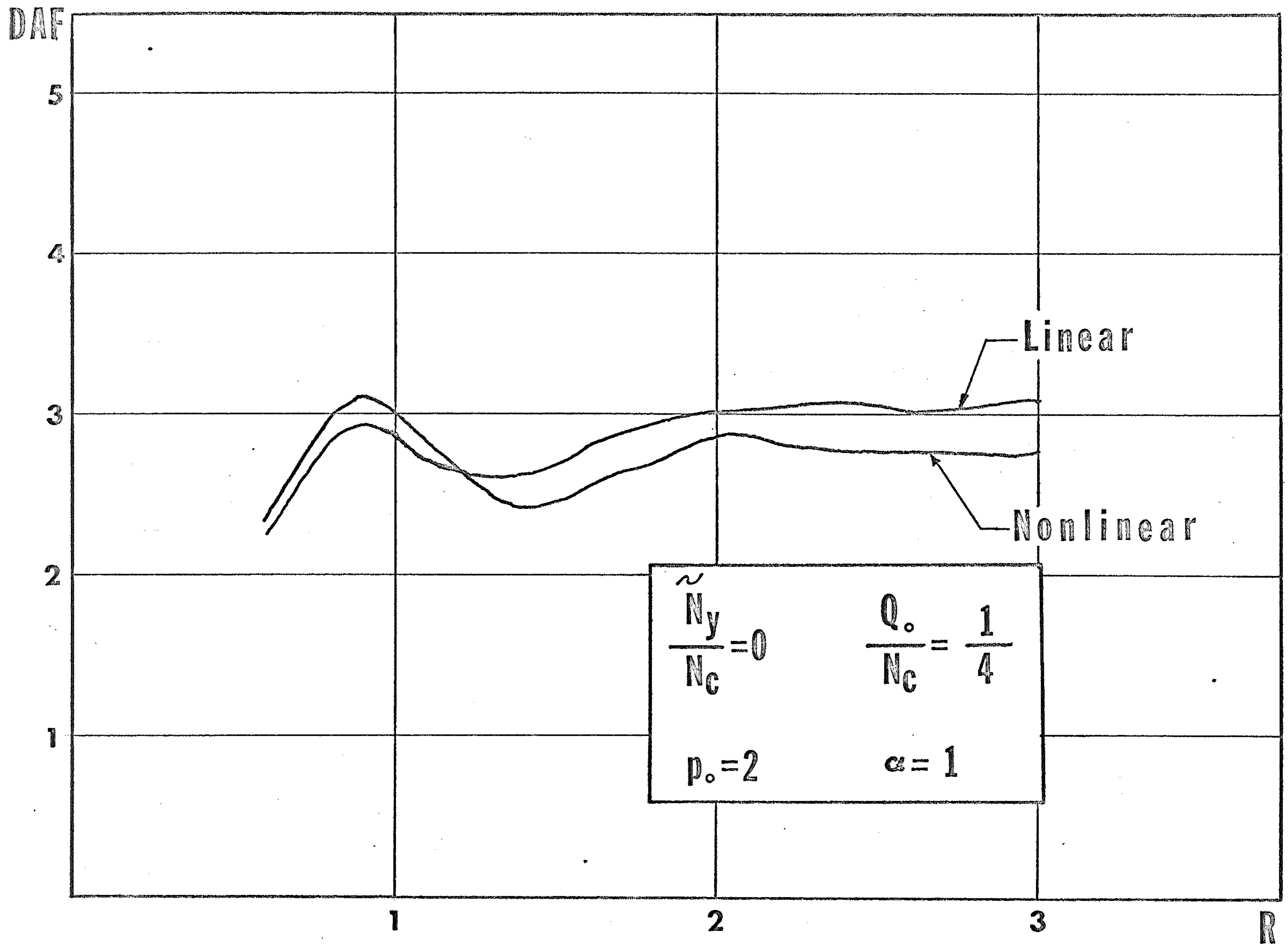

Fig. 13 DAF vs Period Ratio for a Square Plate

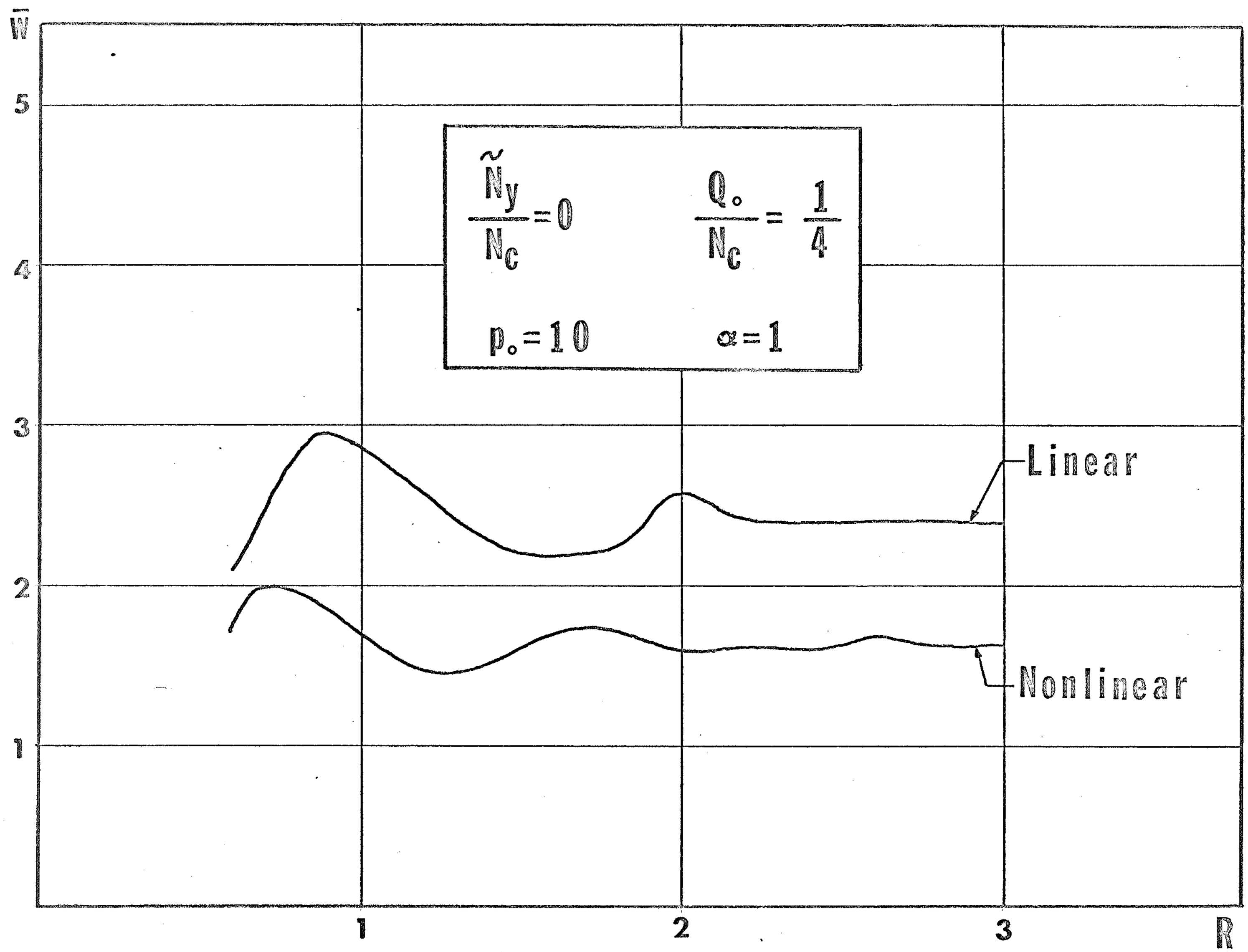

Fig. 14 w vs Period Ratio for a Square Plate

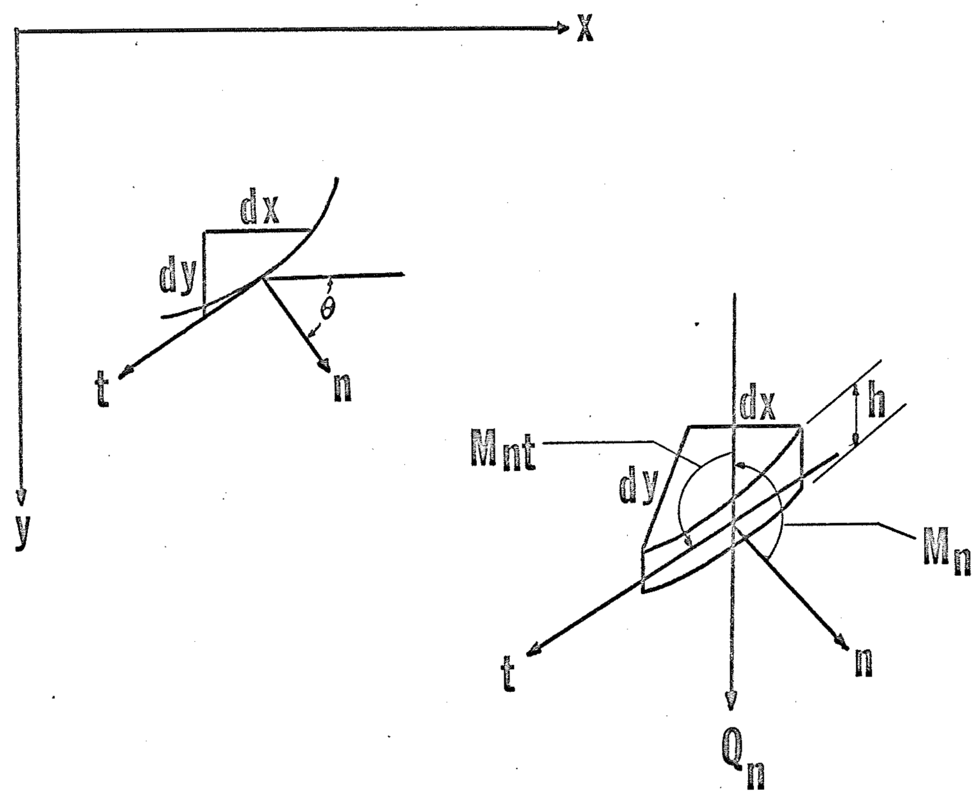

Fig. 15 Sign Convention for Stress Resultants of a Plate

BIBLIOGRAPHY

1. Cheng, D. H. and Benveniste, J. E., "Dynamic Response of Structural Elements Exposed to Sonic Booms", NASA-CR-1281, March 1969.

2. Cheng, D.H. and Benveniste, J.E., "Transient Response of Structural Elements to Traveling Pressure Waves of Arbitrary Shape", Int. J. Mech. Sci., 8, 1966, pp. 607-618.

3. Lowery, L. and Andrews, D. K., "Acoustical and Vibrational Studies Relating to an Occurence of Sonic Boom Induced Damage to a Window in a Store Front", NASA-CR-66170, July 1966.

4. Leissa, A. W., "Vibration of Plates", Chapter 10, NASA SP-160, 1969.

5. Bolotin, V. V., Dynamic Stability of Elastic Systems, Holden-Day, 1964.

6. Somerset, J.H. and Evan-Iwanowski, R. M., "Influence of Non-linear Inertia on the Parametric Response of Rectangular Plates", Int. J. of Non-linear Mech., Vol. 2, 1967.

7. Mathieu, E., "Mémoire sur le mouvement vibration d'une membrane de forme elliptique", Jour. de Math. Pures et Appliquées (Jour. de Liouville), 13, 137, 1868.

8 Floquet, A. M.G., "Sur les équations differentielles lineaires", Ann. de l'Ecole Normale Superieure, 12, 47, 1883.

9. McLachlan, N. W., "Computation of Solution of Mathieu's Equation", Phil Mag., 36, 403, 1945.

BIBLIOGRAPHY (continued)

10. Von Kármán, T., "Festigkeitsprobleme in Maschinenbau", Encyklopädie der mathematischen Wissenschaften, Vol. IV, 4 (1910), Chap. 27, p. 349.

11. Hamilton, W.R., Phil Trans. 1834, p. 307

12. Sokolnikoff, I. S., Mathematical Theory of Elasticity, McGraw-Hill, 1956. p. 413.

13. Hamming, R. W., "Stable Predictor Corrector Methods for Ordinary Differential Equations", J. Assoc. Comp. Mach., Vol. 6, 1959, pp. 37-47

14. Timoshenko, S. and Woinowsky-Krieger, S., Theory of Plates and Shells, McGraw-Hill, 1959.

15. Ralston, A. and Wilf, H. S., Mathematical Methods for Digital Computers, Wiley, 1960, pp. 95-109.

16. Ralston, A., "Runga-Kutta Methods with Minimum Error Bounds", MTAC, Vol. 16, no. 80 (1962), pp. 431-437.

17. McKinley, R. W., "Response of Glass in Windows to Sonic Booms", ASTM Symposium on Effects of Sonic Boom on Buildings, Nov. 1964, pp. 594-600.

18. Herrmann, G. "Influence of Large Amplitudes on Flexural Motions of Elastic Plates", NACA Technical Note 3578, May 1956.